




Targeting the ABC transporter ABCB5 sensitizes glioblastoma to temozolomide-induced apoptosis through a cell-cycle checkpoint regulation mechanism

Received for publication, April 10, 2020, and in revised form, April 10, 2020. Published, Papers in Press, April 20, 2020, DOI 10.1074/jbc.RA120.013778

Catherine A. A. Lee^{‡S1}, Pallavi Banerjee^{S¶1}, Brian J. Wilson^{S||}, Siyuan Wu[‡], Qin Guo^{‡S¶}, Gretchen Berg^{S¶}, Svetlana Karpova^{¶¶}, Ananda Mishra^{‡S}, John W. Lian^{**}, Johnathan Tran^{‡S}, Max Emmerich^S, George F. Murphy^{||**}, Markus H. Frank^{S||††S5}, and  Natasha Y. Frank^{‡S¶||2}

From the [‡]Division of Genetics, the ^{**}Department of Pathology, and the ^{††}Department of Dermatology, Brigham and Women's Hospital, Harvard Medical School, Boston, Massachusetts 02115, the ^STransplant Research Program, Boston Children's Hospital, Harvard Medical School, Boston, Massachusetts 02115, the [¶]Department of Medicine, Veterans Affairs Boston Healthcare System, Boston, Massachusetts 02132, the ^{||}Harvard Stem Cell Institute, Harvard University, Cambridge, Massachusetts 02138, and the ^{S5}School of Medical and Health Sciences, Edith Cowan University, Perth, Western Australia 6027, Australia

Edited by Xiao-Fan Wang

Glioblastoma multiforme (GBM) is a malignant brain tumor with a poor prognosis resulting from tumor resistance to anticancer therapy and a high recurrence rate. Compelling evidence suggests that this is driven by subpopulations of cancer stem cells (CSCs) with tumor-initiating potential. ABC subfamily B member 5 (ABCB5) has been identified as a molecular marker for distinct subsets of chemoresistant tumor-initiating cell populations in diverse human malignancies. In the current study, we examined the potential role of ABCB5 in growth and chemoresistance of GBM. We found that ABCB5 is expressed in primary GBM tumors, in which its expression was significantly correlated with the CSC marker protein CD133 and with overall poor survival. Moreover, ABCB5 was also expressed by CD133-positive CSCs in the established human U-87 MG, LN-18, and LN-229 GBM cell lines. Antibody- or shRNA-mediated functional ABCB5 blockade inhibited proliferation and survival of GBM cells and sensitized them to temozolomide (TMZ)-induced apoptosis *in vitro*. Likewise, in *in vivo* human GBM xenograft experiments with immunodeficient mice, mAb treatment inhibited growth of mutant *TP53*, WT *PTEN* LN-229 tumors, and sensitized LN-229 tumors to TMZ therapy. Mechanistically, we demonstrate that ABCB5 blockade inhibits TMZ-induced G₂/M arrest and augments TMZ-mediated cell

death. Our results identify ABCB5 as a GBM chemoresistance marker and point to the potential utility of targeting ABCB5 to improve current GBM therapies.

Glioblastoma multiforme (GBM)³, the most common primary malignant brain tumor in adults, is associated with poor prognosis and high lethality (1). Patient survival remains dismal owing to therapeutic resistance to clinically approved drugs, such as temozolomide (TMZ) and bevacizumab, and a high rate of tumor recurrence (2–5). Due to the minimal beneficial effects of existing treatment regimens, there is an urgent need for novel therapeutic strategies targeting therapy-resistant cancer subpopulations, which may correspond to GBM cancer stem cells (CSCs) (2, 5).

Studies in human brain cancer models have identified a central role of CSCs in brain tumor initiation, progression, and chemoresistance (3, 5, 6). CD133/PROM1 has been shown by several research groups to enrich for tumor-initiating GBM subpopulations (2, 4, 5). CD133-positive GBM CSCs possess increased tumorigenicity, chemoresistance, and self-renewal capacity in human-to-mouse xenotransplantation experiments and have been shown to correlate with poor clinical outcomes (2, 4, 5, 7). This suggests that specific eradication of the therapy-refractory CD133-positive CSC reservoirs might help to overcome GBM therapeutic resistance.

This work was supported by National Institutes of Health Grant T32 EB016652-05 (to C. A. A. L.); Veterans Affairs BLR&D Grant 1101BX000516 and RR&D Grant 1101RX000989, Merit Review Awards, and a Department of Defense translational team science award (to N. Y. F.); NCI, National Institutes of Health, Grants R01CA113796, R01CA158467, and R01CA138231 (to M. H. F.); and NEI, National Institutes of Health, Grants 1R01EY025794 and R24EY028767 (to M. H. F. and N. Y. F.). N. Y. F. and M. H. F. are co-inventors of the ABCB5-related United States Patent 7,928,202 (Targeting ABCB5 for cancer therapy) assigned to Brigham and Women's Hospital, Boston, Massachusetts, and licensed to Ticeba GmbH (Heidelberg, Germany) and Rheacell GmbH & Co. KG (Heidelberg, Germany). M. H. F. serves as a scientific advisor to Ticeba GmbH and Rheacell GmbH & Co. KG. The content is solely the responsibility of the authors and does not necessarily represent the official views of the National Institutes of Health.

¹ Both authors contributed equally to this work.

² To whom correspondence should be addressed: Brigham and Women's Hospital, 77 Avenue Louis Pasteur, 168F Boston, MA 02115. Tel.: 617-525-4451; Fax: 617-525-5333; E-mail: nyfrank@bwh.harvard.edu.

³ The abbreviations used are: GBM, glioblastoma multiforme; TMZ, temozolomide; ABCB5, ABCB1, and ABCG2, ATP-binding cassette member B5, B1, and G2, respectively; ATM, ataxia telangiectasia mutated; CHEK1, checkpoint kinase 1; CDC25C, cell division cycle 25C; CDK1, cyclin-dependent kinase 1; WEE1, WEE1 G₂ checkpoint kinase; MYT1, myelin transcription factor 1; PLK1, Polo-like kinase 1; TP53, tumor protein P53; IDH, isocitrate dehydrogenase (NADP⁺); PTEN, phosphatase and tensin homology; EGFR, epidermal growth factor receptor; U-87 MG, LN-18, and LN-229, GBM cell lines; CSC, cancer stem cell; LGG, lower-grade glioma; TCGA, The Cancer Genome Atlas; OS, overall survival; MTT, 3-(4,5-dimethylthiazol-2-yl)-2,5-diphenyltetrazolium diphenyltetrazolium bromide; ANOVA, analysis of variance; IPA, ingenuity pathway analysis; KD, knockdown; shRNA, short hairpin RNA; IP, immunoprecipitation; OD, optical density; RIPA, radioimmune precipitation; NSG, NOD/SCID IL2r^{-/-}; PI, propidium iodide; APC, allophycocyanin.

TMZ is a clinically approved drug for the treatment of GBM, which leads to significant prolongation of patient survival (8). Although acting as a cytotoxic imidazotetrazine, TMZ can induce a G₂/M arrest (9, 10), which allows therapy-resistant cancer cells to repair the DNA before entering into the mitotic or M phase, hence protecting the cells and their progeny from drug-induced cytotoxicity (11–13). An essential step for G₂/M transition is activation of the cyclin B1/CDK1 complex. In resting cells, the tyrosine kinases WEE1 and MYT1 induce inhibitory phosphorylation of CDK1, thus maintaining the cyclin B1/CDK1 complex in an inactive state. As the cells prepare to divide, polo-like kinase (PLK1), a major positive regulator of G₂/M transition (14), is activated. Subsequently, PLK1 induces expression of CDK1 by inhibiting WEE1 and MYT1. PLK1 also activates CDC25C, which in turn plays a pivotal role in dephosphorylation and activation of CDK1. Chemotherapeutic drugs and other DNA-damaging agents can severely impair this pathway by activating the sensory ATM/ATR kinases, which phosphorylate and activate CHEK1. CHEK1 phosphorylates and inactivates CDC25C, hence retaining the cyclin B1/CDK1 complex in an inactive phosphorylated state and eventually causing G₂/M arrest. Thus, new approaches to cancer therapeutics aim to use conventional drugs in combination with agents that are capable of abrogating G₂/M arrest (15–17).

Our laboratory has shown that ABC family member B5 (ABCB5) is preferentially expressed by tumor-initiating and therapy-resistant CSC subpopulations in diverse human malignancies, where it is also co-expressed with CD133 (18–22). Recently, ABCB5 was found to be highly up-regulated in the ALDH^{bright} CSC subpopulation in the human U-87 MG GBM cell line (23). Moreover, ABCB5 has been established as a key mediator of tumor growth, aggressiveness, and multidrug resistance in malignant melanoma, colorectal cancer, hepatocellular, oral squamous and Merkel cell carcinomas, and ocular surface squamous neoplasia (18, 21, 24–28). Here, we hypothesized that, similar to its role in other cancers, ABCB5 might contribute to malignant growth and therapy resistance of GBM.

Our study results establish ABCB5 expression in GBM and show that ABCB5 targeting can inhibit tumor growth in human-to-mouse xenotransplantation models and sensitize xenograft tumors to TMZ treatment. Mechanistically, we show that ABCB5 inhibition results in modulation of G₂/M checkpoint regulators and subsequent reversal of TMZ-induced G₂/M arrest, leading to sensitization of GBM to this currently approved therapy.

Results

ABCB5 is expressed in GBM primary tumors and cell lines

We first examined ABCB5 copy number alteration and expression in GBM and lower-grade glioma (LGG) sequencing data from The Cancer Genome Atlas (TCGA) (29). An enhanced increase in copy number gains was seen in GBM (77.4%) compared with oligodendroglioma (19.6%), oligoastrocytoma (22.5%), and astrocytoma (25.3%) (Fig. 1A). There was a statis-

tically significant difference between means of ABCB5 mRNA expression in various brain cancers ($H = 138.1$, $p < 0.0001$). ABCB5 mRNA expression was significantly higher in GBM ($0.51 \pm 0.11 \log_2(\text{counts})$, mean \pm S.E.) compared with oligodendroglioma ($-0.66 \pm 0.05 \log_2(\text{counts})$, $p < 0.0001$), oligoastrocytoma ($-0.62 \pm 0.06 \log_2(\text{counts})$, $p < 0.0001$), and astrocytoma ($-0.64 \pm 0.06 \log_2(\text{counts})$, $p < 0.0001$) (Fig. 1B). There was no statistically significant difference in ABCB5 mRNA expression between oligodendroglioma and oligoastrocytoma ($p > 0.99$), oligoastrocytoma and astrocytoma ($p > 0.99$), or oligodendroglioma and astrocytoma ($p > 0.99$). ABCB5 was detected in the GBM TCGA mRNA expression data set in all three GBM subtypes (classical: $0.16 \pm 0.15 \log_2(\text{counts})$, mesenchymal: $0.90 \pm 0.20 \log_2(\text{counts})$, proneural: $0.48 \pm 0.18 \log_2(\text{counts})$, mean \pm S.E.) (Fig. 1C, left). We also examined the correlation of ABCB5 mRNA expression with overall survival (OS) for all GBM subtypes (Fig. 1C, right). There was a significant trend for median OS to be lower (12.6 versus 14.9 months) for high compared with low ABCB5 expression (optimal cutoff high/low = $\log_2(0.06)$, $p = 0.053$) when all GBM subtypes were considered together. For the mesenchymal subtype, median survival was significantly lower (10.4 versus 15.9 months) for high versus low ABCB5 expression (optimal cutoff = $\log_2(0.92)$, $p = 0.031$). For the classical and the proneural subtypes, median survival was nominally lower, with 14.0 versus 14.9 months (high versus low ABCB5 expression, optimal cutoff = $\log_2(1.55)$, $p = 0.953$) and 12.5 versus 14.9 months (high versus low ABCB5 expression, optimal cutoff = $\log_2(0.03)$, $p = 0.453$), respectively. These results further underscore the clinical significance of ABCB5 expression in GBM, most notably for the mesenchymal subtype. Immunohistochemical analysis confirmed ABCB5 expression in patient-derived primary GBM tumor biopsy material at the protein level (Fig. 1D).

It has been recognized that GBM exhibits substantial inter-tumor heterogeneity and can be distinguished as primary GBM (*i.e.* presenting as fully developed high-grade gliomas without evidence of a precursor lesion) or secondary GBM, which evolves from less malignant astrocytomas (30). Furthermore, recent TCGA analyses identified the existence of distinct GBM molecular subtypes based on their genomic alterations and characteristic molecular signatures (31). Among them, a proneural subtype with mutations in *IDH* and *TP53* corresponds to secondary GBM and is associated with a better outcome (32). A mesenchymal subtype that carries homozygous *PTEN* loss corresponds to primary GBM and is associated with a worse outcome (32, 33). Here, we examined ABCB5 expression and function in GBM cell lines representative of such molecular subtypes (*i.e.* the LN-229 and LN-18 cell lines that carry mutations in *TP53* and are *PTEN* WT and the U-87 MG cell line that is characterized by *PTEN* loss and WT *TP53*) (34). We found ABCB5 to be expressed in all three human GBM cell lines (LN-229, LN-18, and U-87 MG) by quantitative RT-PCR (Fig. 1E), nested RT-PCR (Fig. 1F), and flow cytometric analysis (Fig. 1G), which showed cell surface expression of ABCB5 on 40.6% ($40.6 \pm 0.8\%$, mean \pm S.E.) of LN-229, 31.8% ($31.8 \pm 2.1\%$, mean \pm S.E.) of LN-18, and 16.5% ($16.5 \pm 0.9\%$, mean \pm S.E.) of U-87 MG GBM cells.

ABCB5 targeting sensitizes GBM to temozolomide treatment

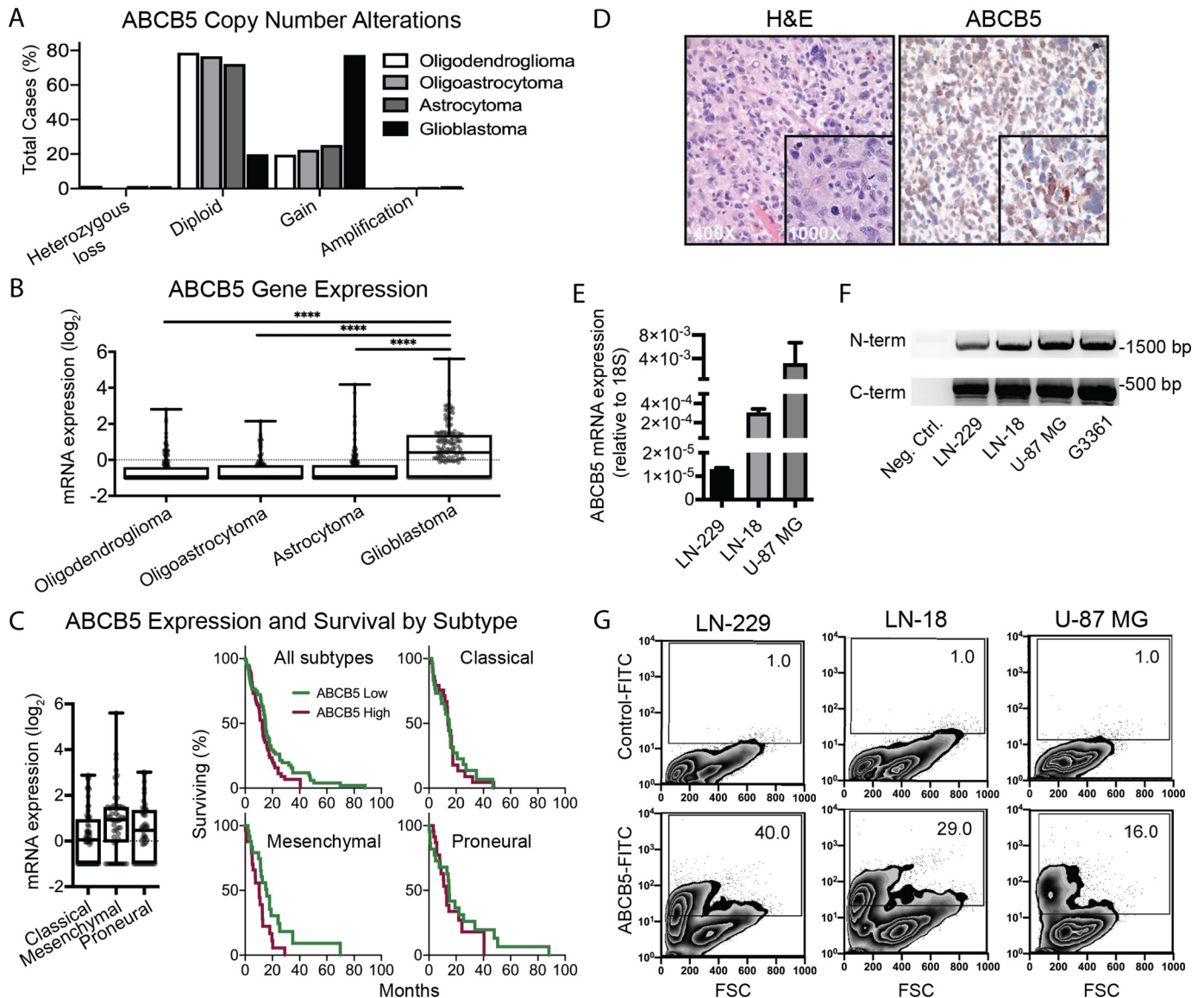


Figure 1. ABCB5 expression in human GBM. *A*, bar graphs depicting copy number alterations as percentage of total cases for GBM ($n = 146$) and LGG (oligodendroglioma: $n = 189$, oligoastrocytoma: $n = 129$, astrocytoma: $n = 194$) brain tumors from TCGA. *B*, box and whisker plot overlaid with individual data points showing the distribution of mRNA expression (\log_2) of ABCB5 in GBM ($n = 152$) and LGG (oligodendroglioma: $n = 191$, oligoastrocytoma: $n = 130$, astrocytoma: $n = 194$) brain tumors from TCGA. Data were analyzed using a Kruskal–Wallis test with Dunn’s multiple-comparison test (****, $p < 0.0001$). Boxes extend from the first quartile to the third quartile; the median is indicated by a solid line. *C*, box and whisker plot (left) overlaid with individual data points showing the distribution of mRNA expression (\log_2) of ABCB5 in the three GBM subtypes (classical: $n = 59$; mesenchymal: $n = 51$; proneural: $n = 46$). Boxes extend from the first quartile to the third quartile; the median is indicated by a solid line. Kaplan–Meier plots (right) depicting OS for all GBM subtypes together ($n = 155$, high events = 58, low events = 65) and each subtype separately (classical: $n = 59$, high events = 24, low events = 24; mesenchymal: $n = 51$, high events = 20, low events = 19; proneural: $n = 66$, high events = 17, low events = 19). OS is expressed in percentage and time in months. *D*, representative immunohistochemical staining for hematoxylin and eosin (H&E) (left) and ABCB5 (right) in clinical GBM. *E*, quantitative RT-PCR of ABCB5 expression from GBM cell lines. Error bars, S.D. (error bars). *F*, nested PCR analysis of ABCB5 mRNA expression in GBM cell lines. G3361, a melanoma cell line, was used as a positive control. Water was used as a negative control. *G*, representative flow cytometric analyses of ABCB5 expression (FITC, FL1 fluorescence) on human GBM cell lines.

ABCB5 is expressed by CD133-positive GBM stem cells, and antibody-mediated ABCB5 blockade reduces the frequency of CD133-positive stem cells

Based on our finding of ABCB5 expression on a subpopulation of GBM cells (Fig. 1G), we hypothesized that ABCB5 might confer therapeutic resistance on GBM CSCs, which are marked by CD133 (2). This hypothesis was supported by previous findings in melanoma and colorectal cancer, where ABCB5 has been shown to be co-expressed with CD133 on therapy-resistant subpopulations of tumor cells (18–22). To test this further,

we first examined CD133 mRNA expression in GBM and LGG RNA-Seq data from TCGA (29). Similar to ABCB5, there was a statistically significant difference in CD133 mRNA expression between means ($H = 71.46$, $p < 0.0001$). CD133 mRNA expression was significantly higher in GBM ($8.39 \pm 0.14 \log_2(\text{counts})$, mean \pm S.E.) compared with oligodendroglioma ($7.21 \pm 0.08 \log_2(\text{counts})$, $p < 0.0001$), oligoastrocytoma ($7.34 \pm 0.08 \log_2(\text{counts})$, $p < 0.0001$), and astrocytoma ($7.64 \pm 0.09 \log_2(\text{counts})$, $p < 0.0001$) (Fig. 2A). There was no statistically significant difference in expression between oligodendroglia-

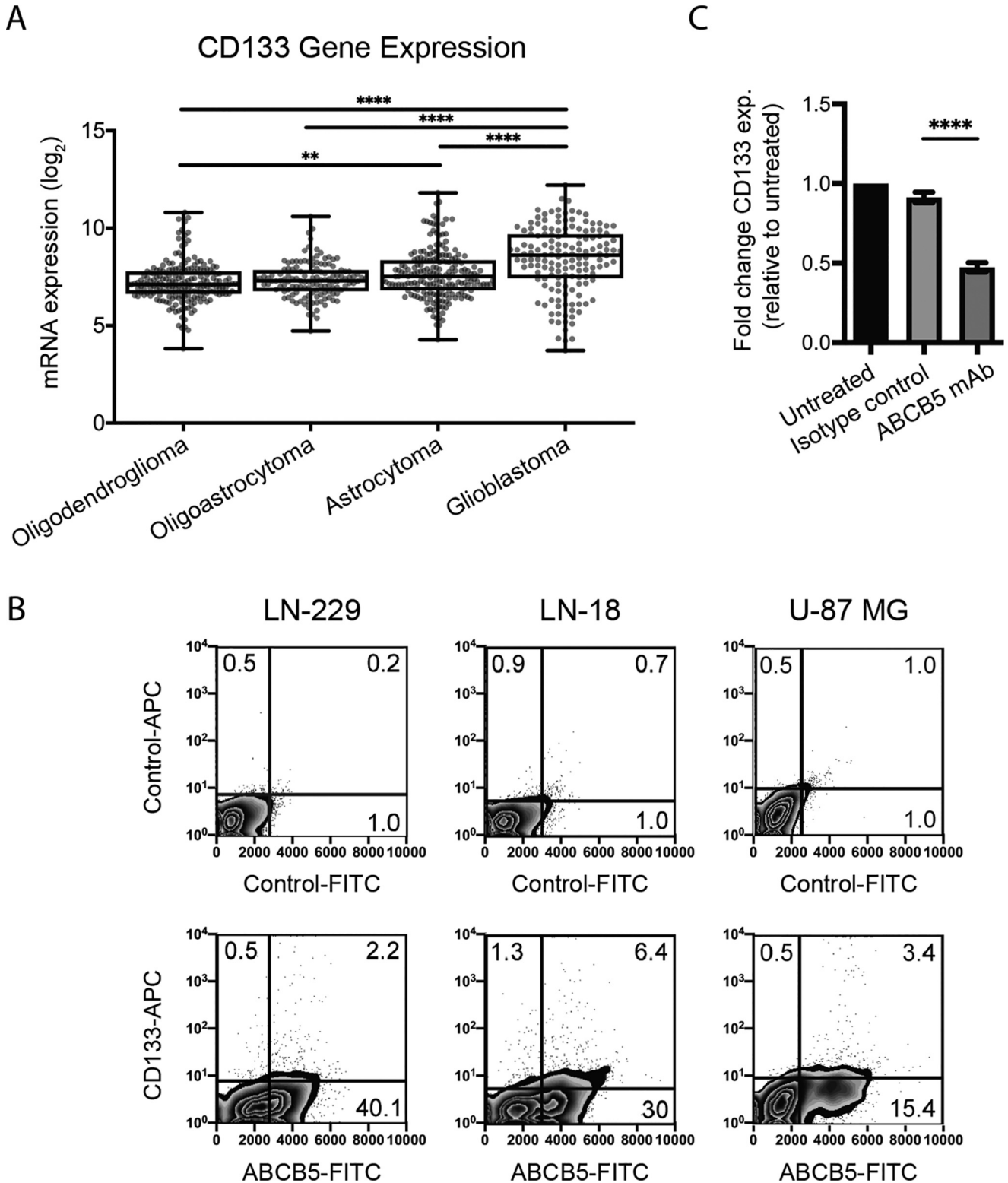


Figure 2. CD133-positive GBM stem cells express ABCB5. *A*, box and whisker plot overlaid with individual data points showing the distribution of mRNA expression (\log_2) of CD133 in GBM ($n = 152$) and LGG (oligodendroglioma: $n = 191$, oligoastrocytoma: $n = 130$, astrocytoma: $n = 194$) brain tumors from TCGA. Data were analyzed using a Kruskal–Wallis test with Dunn’s multiple-comparison test (**, $p < 0.01$; ****, $p < 0.0001$). Boxes extend from the first quartile to the third quartile; the median is indicated by a solid line. *B*, representative dual-color flow cytometric analysis of ABCB5 (FITC, FL1 fluorescence) and CD133 (APC, FL4 fluorescence) co-expression on human GBM cells. Cells co-expressing ABCB5 and CD133 are found in the top right quadrant of each fluorescence plot. Data shown are representative of $n = 3$ independent experiments. *C*, expression of CD133 (APC, FL4 fluorescence) as determined by flow cytometry for LN-229 and LN-18 GBM cell lines. Bar graphs depict -fold change in CD133 positivity relative to untreated control cells. Data analyzed using unpaired t test with Welch’s correction. Error bars, S.E. (error bars) ($n = 6$; ****, $p < 0.0001$).

ABCB5 targeting sensitizes GBM to temozolomide treatment

oma and oligoastrocytoma ($p > 0.99$) or oligoastrocytoma and astrocytoma ($p = 0.40$). Additionally, a statistically significant difference was observed between oligodendroglioma and astrocytoma ($p = 0.004$). CD133 expression positively correlated with ABCB5 in GBM and LGG TCGA RNA-Seq data ($r_s(667) = 0.26$, $p < 0.0001$). Moreover, dual-color flow cytometry confirmed co-expression of ABCB5 and CD133 on 2.2% of LN-229, 6.4% of LN-18, and 3.4% of U-87 MG human GBM cells (Fig. 2B). Furthermore, 100% of CD133-positive LN-229 and U-87 MG cells and 93% of CD133-positive LN-18 cells expressed ABCB5. Considering the evidence for the tumorigenic potential of CD133-positive GBM stem cells (2), expression of ABCB5 on CD133-positive CSCs indicates the possibility of targeting GBM growth by functionally inhibiting ABCB5.

Alongside our recent discovery of a novel anti-apoptotic function of ABCB5 in normal stem cells (35) and human colorectal cancer (18), we hypothesized that ABCB5 might also be required for GBM stem cell maintenance and tumor aggressiveness. When LN-229, LN-18, and U-87 MG cells were incubated with 100 $\mu\text{g}/\text{ml}$ anti-ABCB5 mAb (3C2-1D12) (36) or isotype-matched control mAb for 72 h and expression of CD133 (APC, FL4 fluorescence) was determined by flow cytometry, we found that *in vitro* treatment of the GBM cell lines LN-229 and LN-18 with anti-ABCB5 mAb reduced the frequency of CD133-positive CSC subpopulations by more than 2-fold compared with treatment with isotype control (ABCB5 mAb *versus* isotype control: $0.35 \pm 0.03\%$ *versus* $0.83 \pm 0.03\%$, $p < 0.0001$, mean \pm S.E.) (Fig. 2C), whereas no significant difference in CD133-positive cell frequency was observed in U-87 MG cells after treatment with anti-ABCB5 mAb (ABCB5 mAb *versus* isotype control: $1.24 \pm 0.02\%$ *versus* $1.02 \pm 0.13\%$, $p = 0.1664$, mean \pm S.E.). These differential responses might be explained by the genetic heterogeneity of the GBM cell lines under study. For example, the LN-229 and LN-18 cell lines have increased mutation burden in DNA repair genes, such as *TP53* and WT *PTEN* mutant, compared with U-87 MG, which is a *TP53* WT and *PTEN* mutant. Moreover, these results suggest that, in U-87 MG, CD133-positive GBM stem cells might utilize additional ABCB5-independent pathways for their survival and could show attenuated responses to ABCB5 blockade *in vivo*.

Antibody-mediated ABCB5 blockade inhibits proliferation and promotes apoptosis in human GBM

Considering the significance of CD133-positive CSCs in the growth of GBM, we next examined the effect of the reduction in CSC frequency on GBM cell proliferation. We incubated LN-229, LN-18, and U-87 MG cells with 0–200 $\mu\text{g}/\text{ml}$ ABCB5 mAb or isotype control mAb for 72 h and analyzed cell proliferation by a 3-(4,5-dimethylthiazol-2-yl)-2,5-diphenyltetrazolium diphenyltetrazolium bromide (MTT) assay. There was a statistically significant difference between ABCB5 mAb-treated and isotype control mAb-treated cells as determined by analysis of variance (ANOVA), ($F(1, 144) = 48.42$, $p < 0.0001$). A multiple-comparison test showed that anti-ABCB5 mAb inhibited the proliferation of GBM cells and that this inhibition was statistically significant at concentrations $\geq 20 \mu\text{g}/\text{ml}$ (concentrations, adjusted p values as follows:

20, 0.0293; 50, 0.0021; 100, <0.0001 ; 200, <0.0001) (Fig. 3A). Furthermore, antibody-mediated ABCB5 blockade led to increased apoptosis of GBM cells. LN-229, LN-18, and U-87 MG cells incubated with 100 $\mu\text{g}/\text{ml}$ ABCB5 mAb *versus* isotype-matched control antibody for 72 h showed a 2.3-fold increase in the percentage of apoptotic cells (early + late) (ABCB5 mAb *versus* isotype control: $23.90 \pm 3.5\%$ *versus* $10.55 \pm 1.6\%$, $p < 0.01$, mean \pm S.E.) (Fig. 3B) as determined by dual-color flow cytometry using annexin V (APC, FL4 fluorescence) and propidium iodide (FL2 fluorescence) staining. These results suggest that, similar to its role in normal stem cells (35), ABCB5 serves as a growth-inducing and anti-apoptotic molecule in GBM.

To evaluate the potential role of ABCB5 in GBM growth *in vivo*, we tested the effect of ABCB5 blockade on tumor growth in an established human-to-mouse GBM xenotransplantation model (2, 37). In this experiment, we employed LN-229 and U-87 MG GBM cell lines, which exhibited differential CD133-positive GBM stem cell response to ABCB5 blockade *in vitro*, to test whether this *in vitro* response translates into an *in vivo* effect on tumor growth. The LN-18 cell line was excluded from the *in vivo* study as, consistent with published reports, it reproducibly failed to form tumors (38). LN-229 and U-87 MG GBM cells were injected subcutaneously into immunodeficient NOD/SCID IL2 $\gamma^{-/-}$ (NSG) mice as described (2, 37). Examination of tumor xenografts revealed reduced tumor growth over time after functional blockade of ABCB5 in mice injected with LN-229 GBM cells (Fig. 3C, left). A statistically significant reduction in end point tumor volume was observed for LN-229 (ABCB5 mAb *versus* isotype control: $158.1 \pm 22.26 \text{ mm}^3$ *versus* $68.13 \pm 14.75 \text{ mm}^3$, $p = 0.0098$, mean \pm S.E.) but not U-87 MG GBM cells (ABCB5 mAb *versus* isotype control: $473.3 \pm 156.5 \text{ mm}^3$ *versus* $460.4 \pm 111.7 \text{ mm}^3$, $p = 0.95$, mean \pm S.E.) by unpaired t test. Tumor weight was also decreased in mice treated with anti-ABCB5 mAb compared with isotype control for LN-229 but not U-87 MG GBM cells (ABCB5 mAb *versus* isotype control: LN-229 day 31: $0.315 \pm 0.043 \text{ g}$ *versus* $0.181 \pm 0.032 \text{ g}$, $p = 0.0372$; U-87 MG day 24 (mice sacrificed early due to tumor burden): $0.75 \pm 0.23 \text{ g}$ *versus* $0.724 \pm 0.149 \text{ g}$, $p = 0.926$, mean \pm S.E.) (Fig. 3C, right). These results suggest that GBM tumors might exhibit differential response to mAb-mediated ABCB5 blockade based on their genetic intertumor heterogeneity and divergent growth kinetics.

The growth-inhibitory and pro-apoptotic effects of ABCB5 blockade in LN-229 tumors were further validated by assessing expression of the proliferation marker Ki-67 and apoptosis marker cleaved caspase-3 in tumor xenografts of ABCB5 mAb *versus* isotype control-treated mice. Immunohistochemical analysis (Fig. 3D) of ABCB5 mAb-treated tumor xenografts showed a 2.0-fold decrease in Ki-67 (ABCB5 mAb *versus* isotype control: $22.1 \pm 3.1\%$ *versus* $43.3 \pm 3.2\%$, $p = 0.003$, mean \pm S.E.) (Fig. 3E, left) and a 3.6-fold increase in cleaved caspase-3 (ABCB5 mAb *versus* isotype control: $4.0 \pm 0.4\%$ *versus* $1.1 \pm 0.3\%$, $p = 0.0008$, mean \pm S.E.) (Fig. 3E, right) positive nuclei, underscoring the tumorigenic and anti-apoptotic role of ABCB5 in this GBM model system.

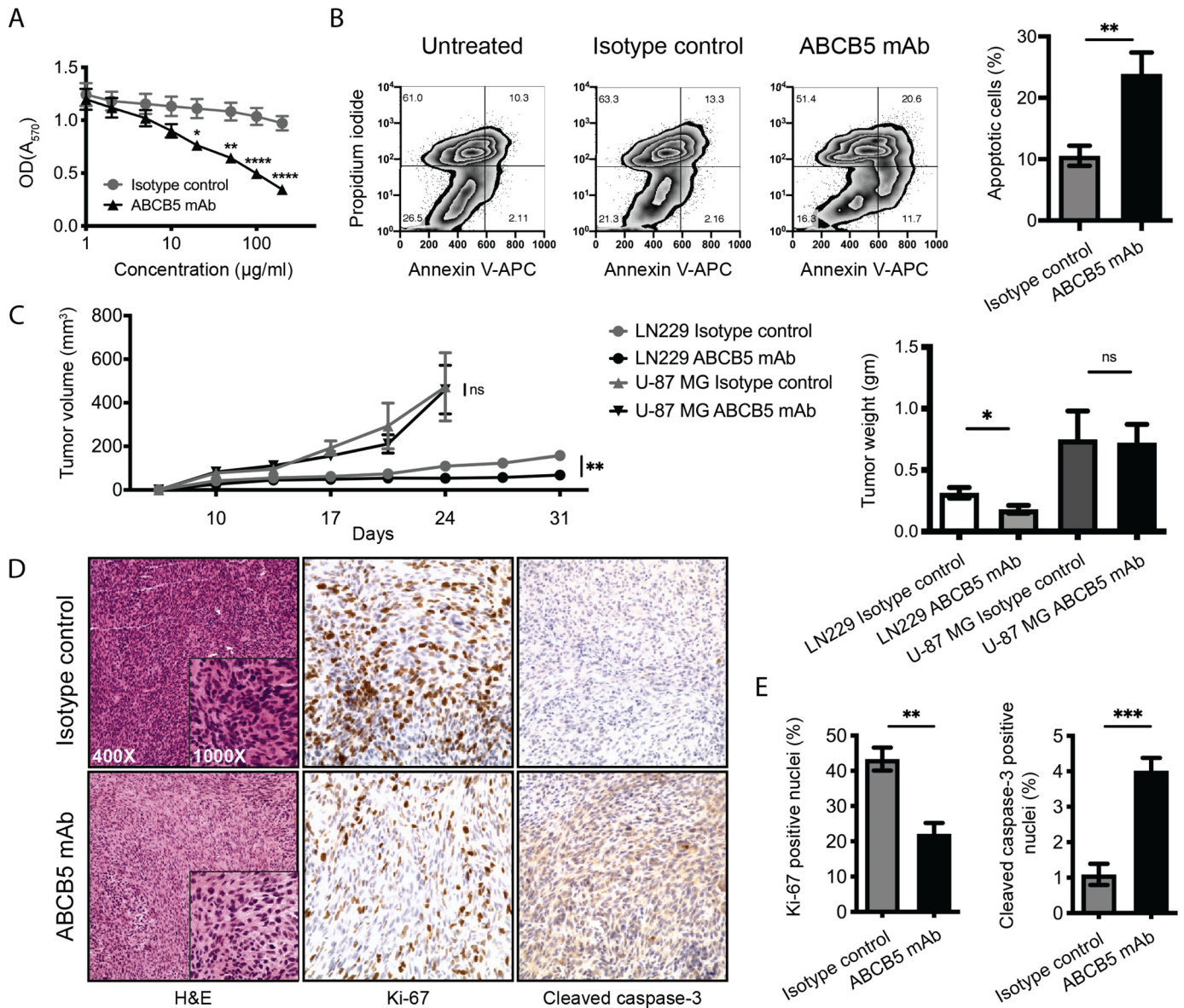


Figure 3. Antibody-mediated ABCB5 blockade inhibits proliferation and induces apoptosis of GBM cells. A, cell proliferation analyzed by MTT assay ($n = 9$). LN-229, LN-18, and U-87 MG GBM cells were incubated with 0–200 $\mu\text{g/ml}$ ABCB5 mAb or isotype control mAb for 72 h. Statistical significance was determined using two-way ANOVA with Sidak's multiple-comparison test (*, $p < 0.05$; **, $p < 0.01$; ****, $p < 0.0001$). Error bars, S.E. (error bars). B, representative plot for the percentage of apoptotic cells as determined by dual-color flow cytometry for LN-229 (left). Cells in early and late apoptotic stages are found in the bottom right and top right quadrant of each fluorescence plot, respectively. Bar graphs show combined data for LN-229, LN-18, and U-87 MG cell lines (right). Data were analyzed using unpaired t test. Error bars, S.E. (**, $p < 0.01$) ($n = 6$). C, *in vivo* tumor growth kinetics (left) of ABCB5 mAb- versus isotype control mAb-treated LN-229 and U-87 MG GBM xenografts ($n = 5$). Statistical significance was determined using unpaired t test (**, $p < 0.01$; ns, not significant). Error bars, S.E. Bar graphs (right) depict mean tumor weight of anti-ABCB5 mAb- versus isotype control mAb-treated LN-229 and U-87 MG GBM xenografts ($n = 5$), analyzed using unpaired t test. Error bars, S.E. (*, $p < 0.05$; ns, not significant). D, representative immunohistochemical staining for Ki-67 and cleaved caspase-3 expression in anti-ABCB5 mAb or isotype control mAb-treated LN-229 GBM xenografts. E, bar graphs represent the percentage of Ki-67-positive (top) or cleaved caspase-3-positive (bottom) nuclei in anti-ABCB5 mAb- versus isotype control mAb-treated GBM tumor xenografts. Data were analyzed using unpaired t test. Error bars, S.E. (**, $p < 0.01$; ***, $p < 0.001$) ($n = 5$).

Targeted ABCB5 blockade augments TMZ-mediated inhibition of GBM cell proliferation and promotes drug-induced apoptosis *in vitro* and *in vivo*

To further dissect a potential role of ABCB5 in GBM therapeutic resistance, we subjected GBM cell cultures to TMZ treatment in combination with mAb-mediated ABCB5 blockade. LN-229, LN-18, and U-87 MG cells were preincubated for 2 h with 100 $\mu\text{g/ml}$ ABCB5 mAb or isotype control mAb and then treated with TMZ (0–1000 μM) for 72 h. A statistically significant reduction in cell proliferation as measured by MTT

assay was observed by ANOVA ($F(1, 160) = 1756, p < 0.0001$), and a multiple-comparison test showed that the inhibitory effect of TMZ on proliferation of GBM cells was further augmented by antibody-mediated blockade of ABCB5 and that this inhibitory effect was statistically significant at all time points measured with the exception of the highest concentration of TMZ (1000 μM) (adjusted p value < 0.0001 for concentrations of $\leq 200 \mu\text{M}$, $p = 0.0101$ at 500 μM) (Fig. 4A). Targeted inhibition of ABCB5 also augmented TMZ-induced apoptosis of GBM cells as determined by dual-color

ABCB5 targeting sensitizes GBM to temozolomide treatment

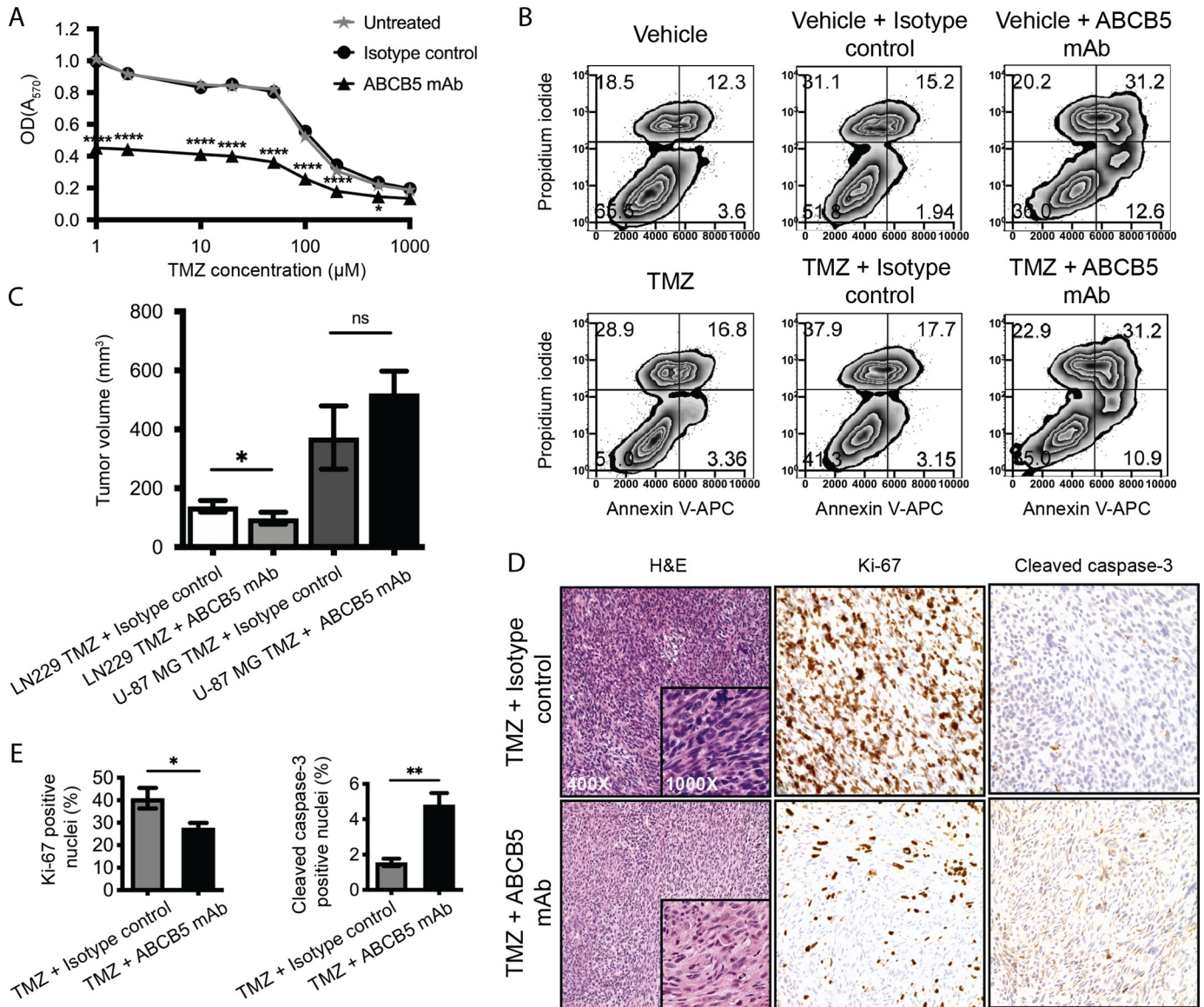


Figure 4. Augmentation of TMZ-induced growth inhibitory effects in GBM by antibody-mediated ABCB5 blockade. *A*, cell proliferation analyzed by MTT assay of LN-229, LN-18, and U-87 MG human GBM cells preincubated for 2 h with 100 $\mu\text{g}/\text{ml}$ ABCB5 mAb or isotype control mAb followed by treatment with TMZ (0–1000 μM) for 72 h ($n = 9$). Error bars, S.E. (error bars) (*, $p < 0.05$; ****, $p < 0.0001$). Statistical significance was determined using two-way ANOVA with Sidak's multiple-comparison test. Error bars, S.E. *B*, percentage of apoptotic cells as determined by dual-color flow cytometry for LN-229. Cells in early and late apoptotic stages are found in the bottom right and top right quadrant of each fluorescence plot, respectively ($n = 3$). *C*, bar graphs represent mean LN-229 or U-87 MG tumor volume of groups treated with TMZ in the presence of ABCB5 mAb or isotype control mAb. Data were analyzed by unpaired *t* test (isotype control: LN-229 ($n = 6$), U-87 MG ($n = 4$); ABCB5 mAb: LN-229 ($n = 6$), U-87 MG ($n = 5$)). Error bars, S.E. (*, $p < 0.05$; ns, not significant). *D*, representative immunohistochemical staining for Ki-67 and cleaved caspase-3 expression in LN-229 GBM xenografts treated with isotype control mAb, ABCB5 vehicle control, or TMZ in the presence of isotype control mAb or ABCB5 mAb. *E*, bar graphs represent the mean percentage of Ki-67- and cleaved caspase-3-positive nuclei of groups treated with TMZ in the presence of ABCB5 mAb or isotype control mAb. Data were analyzed using unpaired *t* test ($n = 5$). Error bars, S.E. (*, $p < 0.05$; **, $p < 0.01$).

flow cytometry using annexin V (APC, FL4 fluorescence) and propidium iodide (FL2 fluorescence) staining. GBM cells preincubated for 2 h with 100 $\mu\text{g}/\text{ml}$ ABCB5 mAb followed by treatment with 100 μM TMZ for 72 h showed an increased percentage (2.3-fold) of apoptotic cells (early + late) compared with those incubated with isotype control mAb (ABCB5 mAb versus isotype control: $43.5 \pm 0.7\%$ versus $18.6 \pm 1.2\%$, $p < 0.0001$, mean \pm S.E.) (Fig. 4*B*), suggesting that ABCB5 might serve as a mediator of TMZ resistance in human GBM.

To test whether mAb-mediated ABCB5 blockade led to sensitization of established GBM tumors *in vivo*, we subjected

LN-229 and U-87 MG xenografted NSG mice to TMZ therapy in the presence of ABCB5 mAb or isotype control. Mice xenografted with LN-229 cells exhibited a 1.4-fold decrease in tumor volume after treatment with TMZ in the presence of ABCB5 mAb compared with mice that received the drug in the presence of isotype-matched control mAb (ABCB5 mAb versus isotype control: $98.50 \pm 20.34 \text{ mm}^3$ versus $138.6 \pm 19.67 \text{ mm}^3$, $p = 0.025$, mean \pm S.E.). Mice xenografted with U-87 MG cells exhibited no significant difference in tumor volume after treatment with TMZ in the presence of ABCB5 mAb compared with mice that received the drug in the presence of isotype-matched control mAb (ABCB5 mAb versus isotype control: $521.7 \pm$

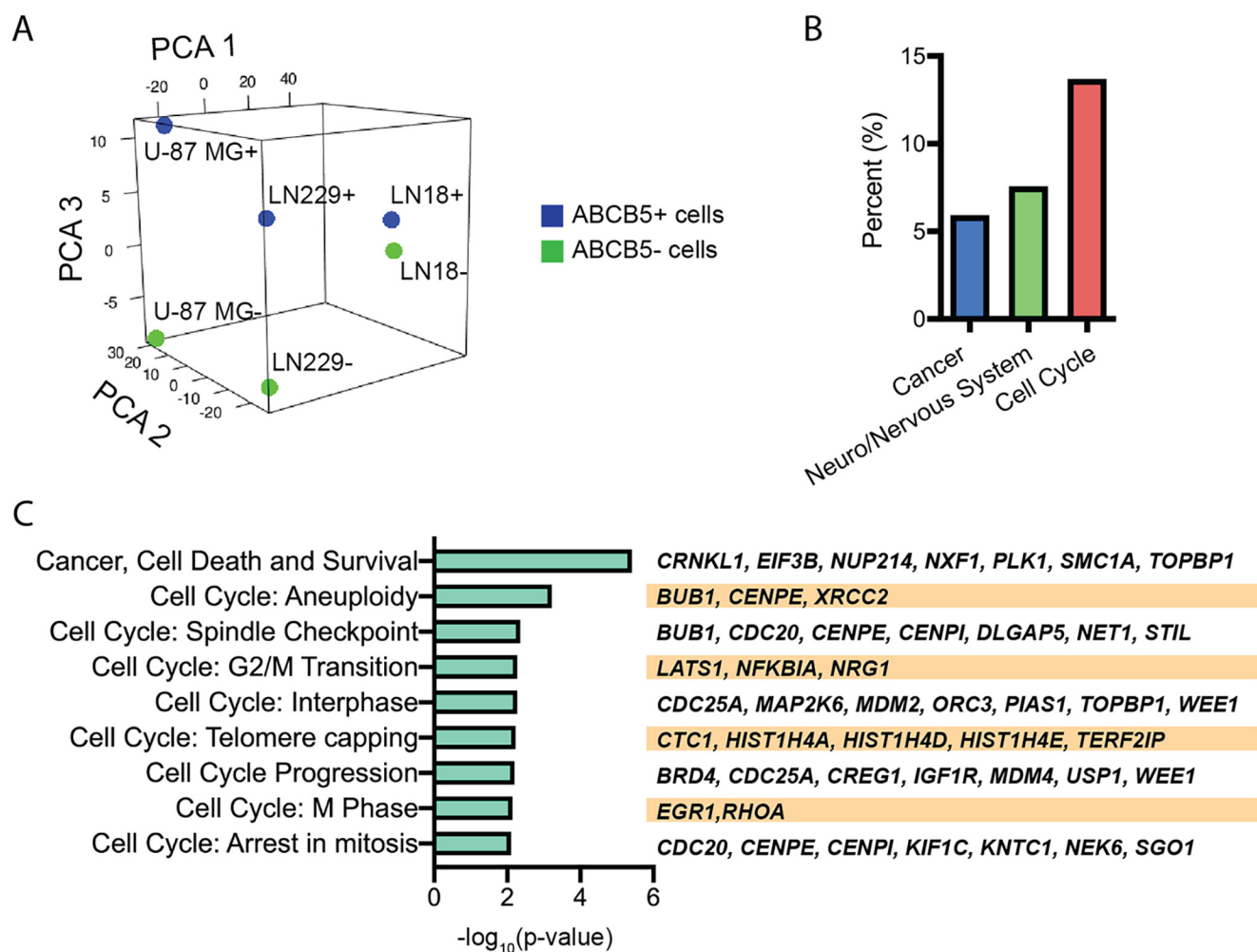


Figure 5. Enrichment of cell cycle-related transcripts in ABCB5-positive GBM cells. A, principal component analysis of all genes detected by microarray analysis of FACS-sorted ABCB5-positive and ABCB5-negative GBM cells ($n = 3$). B, percentage of categories with key words of interest out of 489 total diseases and function categories. C, diseases and functions determined by IPA to be enriched between ABCB5-positive and ABCB5-negative GBM cells ($n = 3$). The p value for a given annotation is calculated by Fisher exact test using the number of focus genes that participate in that process in relation to the total number of genes associated with that process in the IPA knowledgebase. Genes identified by our study listed to the right.

75.52 mm³ versus 372.3 ± 107.4 mm³, $p = 0.059$, mean ± S.E.) (Fig. 4C). Tumors from mice injected with LN-229 cells treated with TMZ in the presence of ABCB5 mAb exhibited a 1.5-fold decrease in Ki-67 (ABCB5 mAb versus isotype control: 27.8 ± 2.1% versus 40.9 ± 4.6%, $p = 0.03$, mean ± S.E.) and a 3.0-fold increase in cleaved caspase-3 (ABCB5 mAb versus isotype control: 4.8 ± 0.6% versus 1.6 ± 0.2%, $p = 0.0013$, mean ± S.E.) (Fig. 4, D and E) positive nuclei compared with isotype control mAb-treated mice. These findings underline the potential role of ABCB5 targeting in the reversal of GBM therapeutic resistance to TMZ and also highlight differential response of GBM tumors to mAb-mediated ABCB5 blockade based on tumor molecular subtype and differences in growth kinetics.

Antibody-mediated blockade of ABCB5 releases GBM cells from TMZ-induced G₂/M arrest

To examine potential molecular mechanisms responsible for the attenuation of GBM tumor growth in the presence of TMZ and mAb-mediated ABCB5 blockade, we performed microarray gene expression analyses of ABCB5-positive and

ABCB5-negative cells sorted by flow cytometry from U-87 MG, LN-18, and LN-229 GBM cell lines. Principal component analysis performed on all genes detected by microarray showed separation specific to the cell lines on PC1 and PC2, whereas PC3 separated the ABCB5-positive and ABCB5-negative cells (Fig. 5A). We generated a list of 1661 genes differentially expressed ($p < 0.05$) between the ABCB5-positive and ABCB5-negative cells in all three cell lines and used this list as input into ingenuity pathway analysis (IPA). IPA determined 489 disease and functional categories to be enriched between the ABCB5-positive and ABCB5-negative cells. Strikingly, 13.7% of these total categories were related to cell cycle (as compared with 5.9% for cancer and 7.6% for neuro/nervous system) (Fig. 5B). Specific enriched categories (reported as $-\log_{10}(p$ value), included Cancer, Cell Death and Survival (5.41), Cell Cycle: Aneuploidy (3.22), Cell Cycle: Spindle Checkpoint (2.36), Cell Cycle: G₂/M Transition (2.28), Cell Cycle: Interphase (2.73), Cell Cycle: Telomere Capping (2.22), Cell Cycle Progression (2.19), and Cell Cycle: M Phase (2.15) (Fig. 5C).

ABCB5 targeting sensitizes GBM to temozolomide treatment

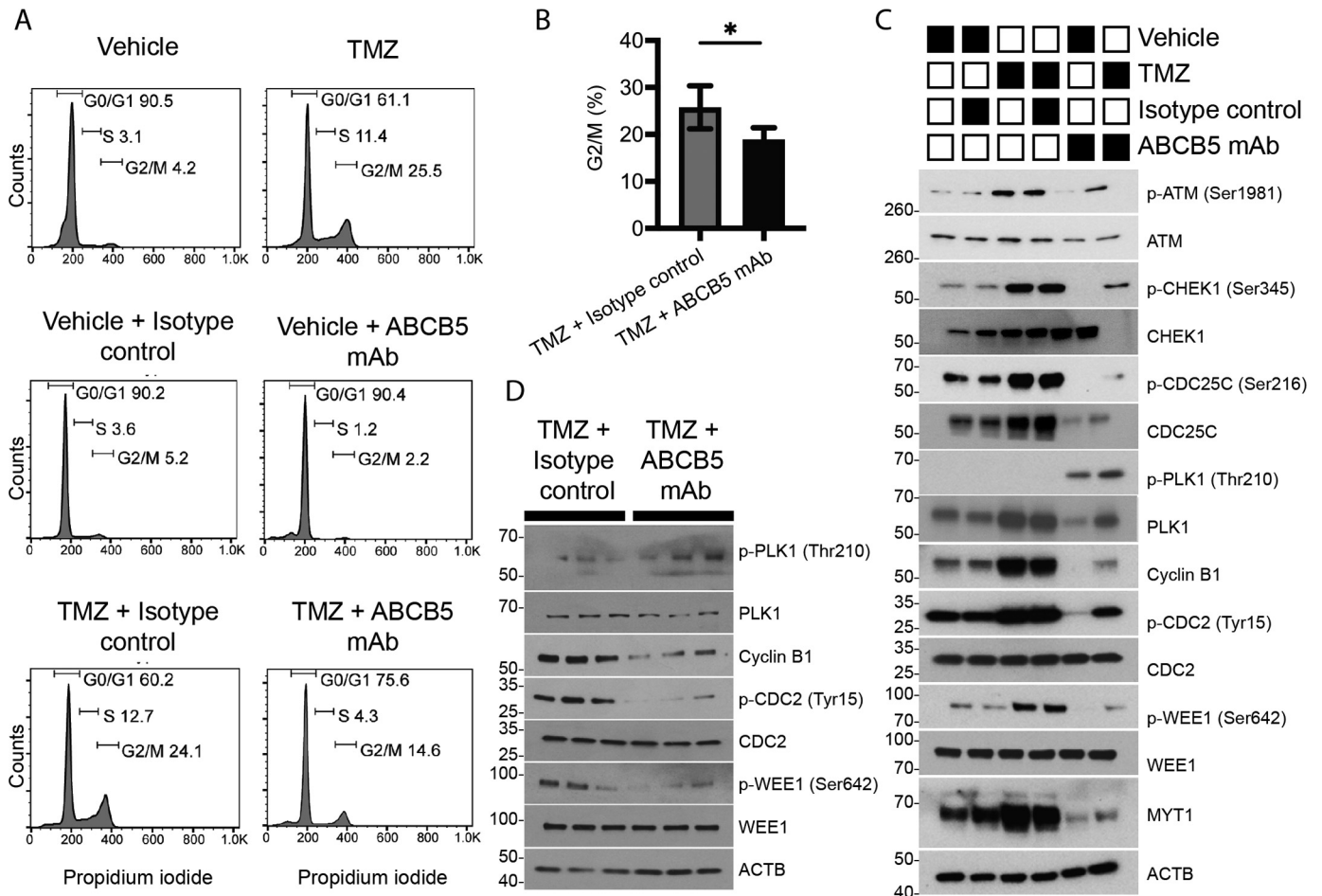


Figure 6. Antibody-mediated ABCB5 blockade releases GBM cells from TMZ-induced G₂/M arrest. *A*, representative flow cytometric DNA content (propidium iodide, FL2 fluorescence) analysis in LN-229 cells following FL2H versus FL2W analysis for doublet elimination. *B*, bar graphs represent percentage of cells in G₂/M arrest from flow cytometry analysis of LN-229, U-87, and LN-18 GBM cells ($n = 8$). Error bars, S.E. (*, $p < 0.05$). *C*, Western blot analysis of cell-cycle checkpoint molecules in LN-229 cells. Molecular weight is indicated to the left (kDa). *D*, Western blot analysis of cell-cycle checkpoint molecules in xenograft tumors from mice treated with TMZ in the presence of anti-ABCB5 mAb or isotype control mAb ($n = 3$). Molecular weight is indicated to the left (kDa).

Based on these results and previous reports showing that TMZ-induced G₂/M cell cycle arrest is responsible for the development of GBM chemoresistance and recurrence (16, 39, 40), we examined whether ABCB5 blockade could reverse GBM chemoresistance through modulation of the G₂/M checkpoint regulators and subsequent reversal of drug-induced G₂/M arrest. LN-229, LN-18, and U-87 MG cells were preincubated for 2 h with 100 μ g/ml ABCB5 mAb or isotype control mAb followed by treatment with 100 μ M TMZ for 72 h. Cells were fixed in ice-cold ethanol and stained in propidium iodide/RNase buffer, and DNA content was analyzed by flow cytometry following FL2H versus FL2W analysis for doublet elimination (Fig. 6A). We found that antibody-mediated functional inhibition of ABCB5 is capable of abrogating TMZ-induced G₂/M arrest in GBM cell cultures, as evidenced by the 1.4-fold reduced cell accumulation in G₂/M phase of the cell cycle following ABCB5 mAb and TMZ treatment, compared with cells that received TMZ treatment in the presence of isotype control (ABCB5 mAb versus isotype control: $18.9 \pm 2.5\%$ versus $25.76 \pm 4.6\%$, $p = 0.0225$, mean \pm S.E.) (Fig. 6B). Western blot analysis revealed that ABCB5 blockade reversed TMZ-mediated G₂/M arrest by inhibiting cell-cycle arrest-inducing checkpoint molecules (ATM, CHK1, WEE1, and MYT1), and

augmenting the activation of molecules that drive cells from G₂ phase to mitosis by either inducing their phosphorylation (as for PLK1) or by removing their inhibitory phosphorylation (as for CDC25C and CDC2) (Fig. 6C). In support of these *in vitro* findings, similar changes in cell cycle protein expression were observed in tumor xenografts from mice treated with TMZ in the presence of either ABCB5 mAb or isotype control mAb (Fig. 6D).

Knockdown of ABCB5 mimics growth inhibition of ABCB5 blockade and releases GBM cells from TMZ-induced G₂/M arrest

Knockdown (KD) of ABCB5 by short hairpin RNA (shRNA) was confirmed by immunoprecipitation (IP)-Western blotting. LN-229 and U-87 MG GBM cells transfected with ABCB5-targeting shRNA showed reduction of ABCB5 protein expression compared with their respective control KD cell variants (LN-229 control KD versus ABCB5 KD: 3.83×10^8 versus 2.15×10^8 integrated density; U-87 MG control KD versus ABCB5 KD: 4.10×10^8 versus 3.34×10^8 integrated density) (Fig. 7A). Similar to antibody-mediated ABCB5 blockade, ABCB5 KD decreased proliferation of LN-229 and U-87 MG GBM compared with their respective control KD cell variants as mea-

ABCB5 targeting sensitizes GBM to temozolomide treatment

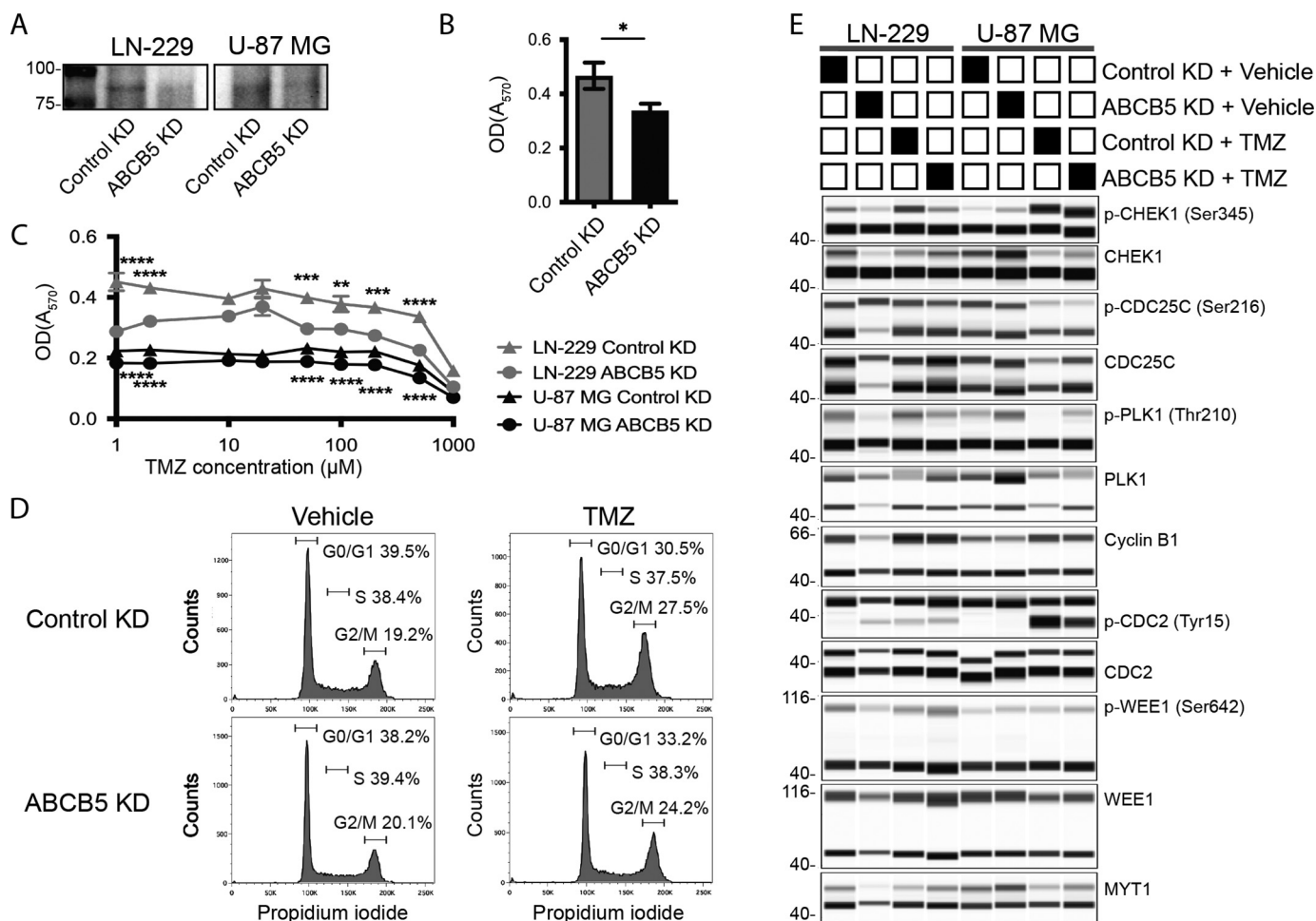


Figure 7. Knockdown of ABCB5 mimics growth-inhibition of ABCB5 blockade and releases GBM cells from TMZ-induced G₂/M arrest. *A*, IP-Western blotting of LN-229 and U-87 MG GBM cells after short hairpin KD. 5 mg of sonicated and precleared protein were loaded per lane. Molecular weight is indicated to the left (kDa). The lanes between LN-229 and U-87 MG were removed for the final figure. *B*, cell proliferation analyzed by MTT assay ($n = 6$). The bar graph represents OD₅₇₀ measurements of LN-229 and U-87 MG GBM cells. Data were analyzed using unpaired *t* test. Error bars, S.E. (*, $p < 0.05$). *C*, cell proliferation analyzed by MTT assay of ABCB5 KD LN-229 or U-87 MG human GBM cells and their corresponding control KD cell variants after treatment with varying concentrations of TMZ (0–1000 μM) for 72 h. Statistical significance was determined using two-way ANOVA followed by Sidak's multiple-comparison test (**, $p < 0.01$; ***, $p < 0.001$; ****, $p < 0.0001$) ($n = 7$). Error bars, S.E. *D*, flow cytometric DNA content (propidium iodide, FL2 fluorescence) analysis in LN-229 cells following FL2H versus FL2W analysis for doublet elimination. *E*, Western blot analysis of cell-cycle checkpoint molecules in LN-229 and U-87 MG GBM cells. The bottom band depicts loading control (ACTB) with the exception of p-CDC2 (Tyr-15) and CDC2 in which ACTB is the top band. Molecular weight is indicated to the left (kDa).

sured by an MTT assay (control KD versus ABCB5 KD: 0.47 ± 0.05 OD₅₇₀ versus 0.34 ± 0.03 OD₅₇₀, $p = 0.0406$, mean \pm S.E.) (Fig. 7B). Treatment of ABCB5 KD and control KD cell lines with TMZ (0–1000 μM) showed a statistically significant reduction in cell proliferation as measured by MTT assay and observed by ANOVA for LN-229 ($F(1,120) = 197.2$, $p < 0.0001$), and a multiple-comparison test showed that the inhibitory effect of TMZ on proliferation of GBM cells was further augmented by antibody-mediated blockade of ABCB5 and that this inhibitory effect was statistically significant at all time points measured with the exception of 10 μM , 20 μM , and the highest concentration of TMZ of 1000 μM (adjusted p value < 0.0001 for 0–2 and 500 μM , $p = 0.0002$ at 50 μM , $p = 0.0041$ at 100 μM , $p = 0.0008$ at 200 μM). This effect was similar for U-87 MG, ANOVA $F(1,119) = 193.3$, $p < 0.0001$), with corresponding results for the multiple-comparison test (adjusted p value < 0.0001 for 1–2 and 50–500 μM , $p = 0.0001$ at 0 μM) (Fig. 7C).

We next used flow cytometry and Western blotting to determine whether KD of ABCB5 releases GBM cells from G₂/M arrest and modulates G₂/M checkpoint regulators. LN-229 ABCB5 KD and control KD GBM cells were treated with 100 μM TMZ for 72 h. Cells were fixed in ice-cold ethanol and stained with propidium iodide/RNase buffer, and DNA content was analyzed by flow cytometry following FL2H versus FL2W analysis for doublet elimination. ABCB5 KD is capable of mitigating TMZ-induced G₂/M arrest in GBM cell cultures, as evidenced by the reduction in cell accumulation in the G₂/M phase of cell cycle following TMZ treatment compared with control KD cells that received TMZ (control KD versus ABCB5 KD: 27.5% versus 24.2%) (Fig. 7D). Similar to the mAb-mediated ABCB5 blockade, shRNA-mediated ABCB5 KD reduced TMZ-induced inhibitory CHEK1 phosphorylation and inhibitory cyclin B1 expression in LN-229 and U-87 MG cells, reduced TMZ-induced inhibitory CDC25 phosphorylation in LN-229 cells, and also reduced TMZ-induced inhibitory CDC2 phos-

ABCB5 targeting sensitizes GBM to temozolomide treatment

phorylation and induced PLK1 phosphorylation in U-87 MG cells (Fig. 7E).

Discussion

In the current study, based on previously established functions in diverse malignancies (18, 21, 24–28), we examined the potential of ABCB5 as a novel therapeutic target in GBM. Our results revealed ABCB5 expression in primary human GBM tumors and three established GBM cell lines. Using mAb-based ABCB5 inhibition strategies *in vitro* or ABCB5 blockade in tumor xenotransplantation models *in vivo*, we show for the first time that targeting ABCB5 can significantly inhibit tumor growth and sensitize a *TP53* mutant *PTEN* WT GBM subtype to TMZ treatment. We demonstrate that ABCB5 inhibition results in modulation of the G_2/M checkpoint regulators and subsequent reversal of TMZ-induced G_2/M arrest.

The finding of specific ABCB5 overexpression in human GBM compared with less aggressive brain tumors and the significant correlation of ABCB5 expression with OS among GBM patients points to a potential role of ABCB5 as a determinant of GBM aggression and therapeutic resistance. This is further supported by the observed expression of ABCB5 on CD133-positive GBM CSCs and a significant positive correlation between CD133 and ABCB5 expression in clinical GBM specimens. CD133-positive GBM subpopulations are enriched for CSCs and exhibit higher rates of self-renewal, proliferation, and tumorigenicity compared with CD133-negative populations (2, 37, 41). Moreover, enrichment of CD133-positive CSCs is observed in GBM cultures, xenografts, and clinical tumor specimens following radiation and chemotherapy (3, 6, 42), highlighting their role in GBM progression and therapy resistance. Our data indicate that, similar to its function in normal tissue stem cells (35), ABCB5 contributes significantly to the survival of GBM CSCs, because antibody-mediated ABCB5 blockade leads to a significant decline in the CD133-positive CSC subpopulation in human GBM cell lines. Our finding that ABCB5 blockade can attenuate proliferation and promote apoptosis underscores the potential role of ABCB5 targeting in the reversal of CSC-mediated GBM tumorigenesis.

Whereas TMZ remains one of the main therapeutic agents in GBM, less than 50% of patients respond to TMZ therapy (43). Here we identified ABCB5 as a potential mechanism of GBM resistance to TMZ. It has been well-established that in GBM, TMZ can induce G_2/M arrest through activation of ATM/ATR-Chk1/2 (9, 10), which is a prosurvival mechanism that enables cancer cells to repair their DNA prior to mitosis entry. Inhibition of the cell-cycle arrest may result in mitotic catastrophe and cell death (16). Our finding of specific enrichment of cell-cycle regulation–related gene categories, such as Cell Cycle: Aneuploidy (3.22), Cell Cycle: Spindle Checkpoint (2.36), and Cell Cycle: G_2/M Transition (2.28), in ABCB5-positive GBM cells (Fig. 5B) suggests that ABCB5 blockade might potentiate growth-inhibitory and pro-apoptotic effects of TMZ through revocation of G_2/M cell cycle arrest.

We found that treatment with TMZ triggered G_2/M arrest in GBM cells by inducing phosphorylation and activation of ATM and CHEK1, inhibitory Ser-216 phosphorylation of CDC25C, retention of inhibitory Tyr-15 phosphorylation of CDK1, acti-

vation of the inhibitory kinases WEE1 and MYT1, and finally, accumulation of cyclin B1, whereas ABCB5 blockade inhibited this arrest-inducing signaling. Treatment of GBM cells with TMZ in the presence of ABCB5 mAb removed the inhibitory phosphorylation of CDC25C and CDK1, thereby activating CDC25C and the cyclin B1/CDK1 complex. This activation of CDC25C and CDK1 triggered by ABCB5 mAb-mediated inhibition of ATM and CHEK1 and by activation of PLK1 that inhibits the inhibitory kinases WEE1 and MYT1 represents a major positive regulator of G_2/M transition (14). Abrogation of the G_2/M checkpoint through inactivation of ATM and CHEK1 has been shown to sensitize GBM and other cancer cells to drug cytotoxicity (16, 44). As a corollary to these reports, our data indicate that attenuation of TMZ-induced G_2/M arrest by ABCB5 blockade sensitized GBM cells to drug-mediated death, as was evident from increased apoptosis and decreased proliferation of GBM cells upon combined treatment with TMZ and ABCB5 mAb. Nevertheless, we cannot exclude the possibility that, in addition to cell-cycle regulation, ABCB5 might also function as a GBM efflux transporter, a function previously attributed to other ABC family members, such as ABCB1 and ABCG2 (45–47). Further studies would be required to investigate this possibility.

Furthermore, several recent studies demonstrated that there is significant intertumor heterogeneity in human GBM and identified GBM molecular subtypes associated with diverse patient outcomes (31–33). Proneuronal or secondary GBM is characterized by mutations in *IDH* and *TP53* with WT *PTEN* status. It has features of neuronal differentiation and is associated with better outcomes (32). Primary GBM possesses a mesenchymal molecular subtype with *EGFR* amplification and *PTEN* loss. It presents at an older age and has worse outcomes (32). Here we found that, whereas ABCB5 blockade exhibited significant anti-tumor activity in all cell lines *in vitro*, the *in vivo* inhibitory effect on tumor growth was more pronounced in *TP53*-mutant *PTEN*-WT LN-229 cells compared with *TP53*-WT *PTEN*-mutant U-87 MG cells. Several factors might be contributing to this differential *in vivo* response. Our recent discoveries that ABCB5 serves as a critical mediator of receptor tyrosine kinase signaling with growth-inducing and anti-apoptotic functions in normal tissues and cancer (35, 48) suggest that constitutive activation of this pathway in the setting of *PTEN* loss in U-87 MG cells can override the effect of ABCB5 blockade. This mechanism might be responsible for the limited impact of ABCB5 blockade on CD133-positive GBM CSC frequency in U-87 MG cells compared with LN-229 and LN-18 cells. As *in vivo* tumor growth is primarily driven by CSC, lack of an inhibitory effect on CSC frequency might also be responsible for the limited *in vivo* effect of ABCB5 inhibition in U-87 MG tumors. Last, the significantly larger tumor sizes in more rapidly growing U-87 MG xenografts could have adversely affected ABCB5 mAb tumor penetration and thus attenuated the effect of ABCB5 blockade on tumor growth. More extensive preclinical studies are needed to further refine ABCB5 targeting strategies for optimal clinical translation.

Our current data define a novel role of ABCB5 in GBM and elucidate a molecular mechanism underlying ABCB5-mediated GBM tumor progression and chemoresistance. They under-

score the potential role of ABCB5 targeting as a novel “two-hit” therapeutic strategy in combating GBM via conferring chemosensitivity as well as targeting those very subpopulations that drive tumor growth.

Experimental procedures

GlioVis

Glioblastoma and lower-grade glioma adult brain tumor copy number alteration and RNA-Seq data sets from TCGA were queried for ABCB5 and PROM1 (CD133), whereas glioblastoma survival and patient outcomes based on subtype were queried for ABCB5 expression from RNA-Seq data sets (29). All human studies were approved by the Institutional Review Board of Partners HealthCare, and the studies abide by the Declaration of Helsinki principles.

Cell culture

Authenticated human GBM cell lines U-87 MG, LN-18, and LN-229 were obtained from American Type Culture Collection (ATCC, Manassas, VA). LN-18 and LN-229 were cultured in Dulbecco’s modified Eagle’s medium, and U-87 MG was cultured in Eagle’s minimum essential medium (ATCC, Manassas, VA) supplemented with 10% (v/v) FBS (Invitrogen GIBCO, Waltham, MA) and 1% (v/v) penicillin/streptomycin (Lonza Bio-Whittaker, Walkersville, MD). For antibody-mediated inhibition of ABCB5, GBM cells were incubated with designated doses of anti-ABCB5 mAb (clone 3C2-1D12) (36) or MOPC31C isotype control mAb (Sigma–Aldrich) for 72 h. All experiments were performed with cell lines that tested negative for mycoplasma (Lonza, Portsmouth, NH).

RNA extraction and RT-PCR

RNA was prepared from U-87 MG, LN-18, and LN-229 GBM or G3361 melanoma cells using a RNeasy Plus isolation kit (Qiagen, Germantown, MD) and reverse-transcribed using an Advantage RT-for-PCR Kit (Clontech, Mountain View, CA) according to the manufacturer’s instructions. cDNA was then subjected to PCR amplification of the full ABCB5 ORF (transcript variant 2, mRNA NCBI reference sequence: NM_178559.5) as described previously for human skin cells (31), using equivalent oligonucleotides ORF-forward (ATG-GTGGATGAGAATGACATCAGAG) and ORF-reverse (AAC-TGCTTTACAAGCAAATGTGCTAG). For sequencing reactions, the PCR product was then used as a template for nested PCR of three overlapping fragments encompassing the ORF: N-terminal, forward (ATGGTGGATGAGAATGACATCAGAGCTTT) and reverse (GAATTAAATAGGCTCCAAATCGAAACCTT); middle, forward (AATGACTGGATTTGCCAACAAAGATA-AGC) and reverse (TTCTCAGGGAGACCTTCAATAAAAAGA-ATG); and C-terminal, forward (AAATAG CAATCGTTCCTC-AAGAGCCTGTG) and reverse (TCACTGCACTGACTGTGC-ATTCACCTAACT). All PCRs used Q5 high-fidelity polymerase (New England Biolabs). The full ORF sequences of ABCB5 (transcript variant 2, mRNA NCBI reference sequence: NM_178559.5) expressed by the human LN-229, LN-18, and U-87 MG glioblastoma cell lines were submitted to the GenBank™ database under the following accession numbers: MK803369, MK803368, MK803366, and MK803367.

Flow cytometric analyses of ABCB5 and CD133 expression

U-87 MG, LN-18, and LN-229 GBM cells were harvested with Versene (Invitrogen GIBCO) and stained with FITC-conjugated mouse monoclonal anti-ABCB5 antibody (clone 3C2-1D12) (21, 36) or CFS-conjugated mouse IgG1 isotype control (R&D Systems, Minneapolis, MN) and APC-conjugated CD133/2 (293C3) (Miltenyi Biotech, Cambridge, MA) or APC-conjugated mouse isotype control (R&D Systems).

Generation of stable ABCB5 knockdown glioblastoma cell variants

Generation of stable LN-229 and U-87 MG ABCB5 KD or their respective shControl cell variants was accomplished described (18, 48), followed by puromycin selection (2 μ g/ml). Reduction of ABCB5 protein expression in ABCB5 KD cell lines was confirmed by IP-Western blotting. Briefly, 5 mg each of sonicated and precleared total cell lysates were prepared in RIPA buffer (Boston BioProducts, Ashland, MA) plus protease inhibitor (Sigma–Aldrich) before incubation with 2 μ g of anti-ABCB5 rabbit polyclonal antibody (Abgent/Abcepta, San Diego, CA) with protein A/G–agarose for 3 h at 4 °C. After washing three times, SDS-PAGE and Western blotting was performed, using the same antibody.

Cell proliferation assay

Cell proliferation was measured by an MTT Cell Proliferation Assay Kit (Trevigen, Gaithersburg, MD) following the manufacturer’s protocol. Briefly, 1×10^4 cells were seeded in 100 μ l of culture medium per well of 96-well plates. Following treatment with anti-ABCB5 mAb or isotype control mAb in the absence or presence of TMZ, 10 μ l of MTT reagent was added to each well. Once purple crystals of formazan were visible, 100 μ l of detergent reagent was added, and the cells were incubated in the dark for 2–4 h until the crystals became soluble. Absorbance was measured at 570 nm and corrected against blank wells, which consisted of culture medium alone and were processed in the same way as above.

In vivo tumor xenograft study

6-Week-old female NSG mice purchased from the Jackson Laboratory (Bar Harbor, ME) were maintained in accordance with the institutional guidelines of Boston Children’s Hospital and Harvard Medical School, and experiments were carried out according to approved experimental protocols. Human xenografts were established by subcutaneous injection of human GBM LN-229 and U-87 MG cells into the right flank of recipient NSG mice (5×10^6 cells/inoculum). For determining the effect of ABCB5 blockade on tumor growth, the mice were injected intraperitoneally with 1 mg of anti-ABCB5 mAb or 1 mg of isotype control mAb three times per week starting 1 week prior to tumor inoculation. To determine the effect of ABCB5 blockade on TMZ (Sigma–Aldrich) sensitization of the xenograft tumors, LN-229 GBM xenografts were established in NSG mice as described above. Once the tumors reached the volume of 100 mm³, the mice were randomized into four groups ($n = 6$ /group) that received either 1 mg of anti-ABCB5 mAb or 1 mg of isotype control mAb in the presence of either 0.1 mg of TMZ

ABCB5 targeting sensitizes GBM to temozolomide treatment

or its vehicle. Intraperitoneal injection of anti-ABCB5 mAb or the isotype control mAb was started a week before the initiation of daily intraperitoneal injections of TMZ. TMZ was freshly dissolved in 10% DMSO and diluted in saline before every injection. Tumor volumes were measured twice every week according to the established formula, tumor volume (mm^3) = $\pi/6 \times 0.5 \times \text{length} \times (\text{width})^2$ (24). All experimental procedures were reviewed and approved by Boston Children's Hospital and the Veterans Affairs Boston Animal Care and Use Committee.

Immunohistochemistry

Immunohistochemical staining for Ki-67 and cleaved caspase-3 on deparaffinized 5- μm sections of GBM tumor xenografts was done as described previously (18), using anti-Ki-67 (Vector Laboratories, Burlingame, CA) and anti-cleaved caspase-3 (Cell Signaling Technology, Danvers, MA) antibodies. For quantitative analyses of Ki-67 and cleaved caspase-3 expression in the xenograft tumors, slides were scanned via the Aperio Digital Pathology Service provided by the Research Pathology Cores, Dana-Farber/Harvard Cancer Center (Boston, MA). Nuclear staining algorithms were utilized for enumeration of the positive cells.

Apoptosis assay

GBM cells were treated with anti-ABCB5 mAb or isotype control mAb in the absence or presence of TMZ for 72 h. Induction of apoptosis by antibody-mediated ABCB5 blockade was detected by flow cytometry using APC annexin V and PI (BD Biosciences) staining as per the manufacturer's protocol.

Microarray analyses

Microarray analyses were performed by the Microarray Core Facility at the Dana-Farber Cancer Institute using HTA 2.0 human arrays. FACS-sorted ABCB5-positive and ABCB5-negative cells isolated from U-87 MG, LN-18, and LN-229 GBM cell lines were compared. Data were preprocessed using the R Bioconductor oligonucleotide package (49) with the RMA normalization method. Differentially expressed genes were identified using the R Bioconductor *limma* package (50, 51) with predefined criteria, followed by input of these genes into Ingenuity Pathway Analysis (52).

Cell cycle analysis

Cell cycle distribution was determined by flow cytometry using PI/RNase staining buffer (BD Biosciences) following the manufacturer's protocol. Briefly, harvested cells were washed in PBS and fixed in ice-cold 70% ethanol overnight. The fixed cells were washed in PBS and resuspended in PI/RNase staining buffer. Following incubation at 37 °C for 30 min, the fractions of cells in G₀/G₁, S, and G₂/M phase were analyzed by flow cytometry at an excitation wavelength of 488 nm and an emission wavelength of 630 nm (53).

Western blotting

Protein lysates were prepared from cultured GBM cells or excised human GBM xenograft tumors in RIPA buffer (Cell Signaling Technology, Danvers, MA) supplemented with protease inhibitor mixture (Sigma–Aldrich). Normalized protein

lysates were run on SDS-polyacrylamide gels and transferred to a polyvinylidene difluoride membrane (GE Healthcare). The membranes were incubated with either rabbit anti- β -actin (D6A8), mouse anti- β -actin (8H10D10), anti-phospho-ATM (Ser-1981) (D6H9), anti-ATM (D2E2), anti-phospho-CHEK1 (Ser-345) (133D3), anti-CHEK1 (2G1D5), anti-phospho-CDC25C (Ser-216) (63F9), anti-CDC25C (5H9), anti-phospho-PLK1 (Thr-210) (D5H7), anti-PLK1 (208G4), anti-cyclin B1 (D5C10), anti-phospho-CDC2 (Tyr-15) (10A11), anti-CDC2, anti-phospho-WEE1 (Ser-642) (D47G5), anti-WEE1 (D10D2), or anti-MYT1 (Cell Signaling Technology, Danvers, MA) and subsequently incubated with peroxidase-linked secondary antibody. The reactive bands were detected using chemiluminescent substrate (Thermo Scientific).

Capillary Western blotting analyses

Capillary Western analyses were performed on a Western blotting system (ProteinSimple) according to the manufacturer's instructions. In brief, protein lysates were prepared from cultured GBM cells in RIPA buffer and diluted to 2 $\mu\text{g}/\mu\text{l}$ in sample buffer. The diluted samples were combined with fluorescent master mix and heated for 5 min at 95 °C. The prepared samples, blocking reagent, primary antibodies (1:20 dilution for CDC25C, PLK1, cyclin B1, CDC2, WEE1, and MYT1; 1:10 dilution for CHEK1; 1:5 dilution for phospho-CHEK1, phospho-CDC25C, phospho-PLK1, phospho-CDC2, and phospho-WEE1; and 1:80 dilution for mouse and rabbit β -actin), secondary antibodies, and chemiluminescent substrate were pipetted into designated wells in the assay plate. The electrophoresis and immunodetection steps were carried out in the fully automated capillary system. Data were analyzed using Compass software (ProteinSimple).

Statistics

The data are expressed as mean \pm S.E. of three or more independent experiments. A Kruskal–Wallis test with Dunn's multiple-comparison test with a single pooled variance was used to determine statistically significant difference in the TCGA RNA-Seq data, with $p < 0.05$ considered significant. To determine the cutoff between high and low ABCB5 expression in the GBM RNA-Seq data and for the different GBM subtypes, the R package *maxstat* was used to identify the cut point based on the maximally selected rank statistic. Statistically significant difference in expression level of markers, percentage of apoptotic cells, DNA content of cells, and tumor weight between different groups was determined by unpaired and paired *t* test, with $p < 0.05$ considered significant. Statistically significant difference in cell growth kinetics or tumor growth kinetics between different groups was determined using two-way ANOVA and Sidak's multiple-comparison test, with $p < 0.05$ considered significant.

Data availability

The full ORF sequences of ABCB5 (transcript variant 2, mRNA NCBI reference sequence: NM_178559.5) expressed by the human LN-229, LN-18, and U-87 MG glioblastoma cell lines were submitted to the GenBank™ database under the following accession numbers: MK803369, MK803368,

MK803366, and MK803367. The microarray analyses were deposited to the Gene Expression Omnibus under accession number GSE127895.

Author contributions—C. A. A. L., P. B., B. J. W., M. H. F., and N. Y. F. conceptualization; N. Y. F. resources; C. A. A. L., P. B., B. J. W., S. W., G. F. M., M. H. F., and N. Y. F. data curation; C. A. A. L., P. B., B. J. W., G. F. M., M. H. F., and N. Y. F. formal analysis; N. Y. F. supervision; N. Y. F. funding acquisition; C. A. A. L. and N. Y. F. validation; C. A. A. L., P. B., B. J. W., S. W., Q. G., G. B., S. K., A. M., J. W. L., J. T., M. E., G. F. M., M. H. F., and N. Y. F. investigation; C. A. A. L., B. J. W., S. W., and N. Y. F. methodology; C. A. A. L., P. B., B. J. W., and N. Y. F. writing—original draft; C. A. A. L., M. H. F., and N. Y. F. writing—review and editing.

References

- Back, M., Rodriguez, M., Jayamanne, D., Khasraw, M., Lee, A., and Wheeler, H. (2016) Understanding the Revised Fourth Edition of the World Health Organization Classification of Tumours of the Central Nervous System for Clinical Decision-making: A Guide for Oncologists Managing Patients with Glioma. *Clin. Oncol. (R. Coll. Radiol.)* **30**, 556–562 [CrossRef Medline](#)
- Singh, S. K., Hawkins, C., Clarke, I. D., Squire, J. A., Bayani, J., Hide, T., Henkelman, R. M., Cusimano, M. D., and Dirks, P. B. (2004) Identification of human brain tumour initiating cells. *Nature* **432**, 396–401 [CrossRef Medline](#)
- Chen, J., Li, Y., Yu, T. S., McKay, R. M., Burns, D. K., Kernie, S. G., and Parada, L. F. (2012) A restricted cell population propagates glioblastoma growth after chemotherapy. *Nature* **488**, 522–526 [CrossRef Medline](#)
- Liu, G., Yuan, X., Zeng, Z., Tunic, P., Ng, H., Abdulkadir, I. R., Lu, L., Irvin, D., Black, K. L., and Yu, J. S. (2006) Analysis of gene expression and chemoresistance of CD133+ cancer stem cells in glioblastoma. *Mol. Cancer* **5**, 67 [CrossRef Medline](#)
- Lathia, J. D., Mack, S. C., Mulkearns-Hubert, E. E., Valentim, C. L., and Rich, J. N. (2015) Cancer stem cells in glioblastoma. *Genes Dev.* **29**, 1203–1217 [CrossRef Medline](#)
- Bao, S., Wu, Q., McLendon, R. E., Hao, Y., Shi, Q., Hjelmeland, A. B., Dewhirst, M. W., Bigner, D. D., and Rich, J. N. (2006) Glioma stem cells promote radioresistance by preferential activation of the DNA damage response. *Nature* **444**, 756–760 [CrossRef Medline](#)
- Zeppernick, F., Ahmadi, R., Campos, B., Dictus, C., Helmke, B. M., Becker, N., Lichter, P., Unterberg, A., Radlwimmer, B., and Herold-Mende, C. C. (2008) Stem cell marker CD133 affects clinical outcome in glioma patients. *Clin. Cancer Res.* **14**, 123–129 [CrossRef Medline](#)
- Stupp, R., Mason, W. P., van den Bent, M. J., Weller, M., Fisher, B., Taphoorn, M. J., Belanger, K., Brandes, A. A., Marosi, C., Bogdahn, U., Curschmann, J., Janzer, R. C., Ludwin, S. K., Gorlia, T., Allgeier, A., et al. (2005) Radiotherapy plus concomitant and adjuvant temozolomide for glioblastoma. *N. Engl. J. Med.* **352**, 987–996 [CrossRef Medline](#)
- Newlands, E. S., Stevens, M. F., Wedge, S. R., Wheelhouse, R. T., and Brock, C. (1997) Temozolomide: a review of its discovery, chemical properties, pre-clinical development and clinical trials. *Cancer Treat. Rev.* **23**, 35–61 [CrossRef Medline](#)
- Filippi-Chiela, E. C., Thomé, M. P., Bueno e Silva, M. M., Pelegrini, A. L., Ledur, P. F., Garicochea, B., Zamin, L. L., and Lenz, G. (2013) Resveratrol abrogates the temozolomide-induced G₂ arrest leading to mitotic catastrophe and reinforces the temozolomide-induced senescence in glioma cells. *BMC Cancer* **13**, 147 [CrossRef Medline](#)
- DiPaola, R. S. (2002) To arrest or not to G₂-M cell-cycle arrest: commentary re: A. K. Tyagi et al., Silibinin strongly synergizes human prostate carcinoma DU145 cells to doxorubicin-induced growth inhibition, G₂-M arrest, and apoptosis. *Clin. Cancer Res.* **8**, 3311–3314 [Medline](#)
- Sherr, C. J. (2000) The Pzcoller lecture: cancer cell cycles revisited. *Cancer Res.* **60**, 3689–3695 [Medline](#)
- Schwartz, G. K., and Shah, M. A. (2005) Targeting the cell cycle: a new approach to cancer therapy. *J. Clin. Oncol.* **23**, 9408–9421 [CrossRef Medline](#)
- van Vugt, M. A., and Medema, R. H. (2005) Getting in and out of mitosis with Polo-like kinase-1. *Oncogene* **24**, 2844–2859 [CrossRef Medline](#)
- Jackson, J. R., Gilmartin, A., Imburgia, C., Winkler, J. D., Marshall, L. A., and Roshak, A. (2000) An indolocarbazole inhibitor of human checkpoint kinase (Chk1) abrogates cell cycle arrest caused by DNA damage. *Cancer Res.* **60**, 566–572 [Medline](#)
- Hirose, Y., Berger, M. S., and Pieper, R. O. (2001) Abrogation of the Chk1-mediated G₂ checkpoint pathway potentiates temozolomide-induced toxicity in a p53-independent manner in human glioblastoma cells. *Cancer Res.* **61**, 5843–5849 [Medline](#)
- Tyagi, A. K., Singh, R. P., Agarwal, C., Chan, D. C., and Agarwal, R. (2002) Silibinin strongly synergizes human prostate carcinoma DU145 cells to doxorubicin-induced growth inhibition, G₂-M arrest, and apoptosis. *Clin. Cancer Res.* **8**, 3512–3519 [Medline](#)
- Wilson, B. J., Schatton, T., Zhan, Q., Gasser, M., Ma, J., Saab, K. R., Schanche, R., Waaga-Gasser, A. M., Gold, J. S., Huang, Q., Murphy, G. F., Frank, M. H., and Frank, N. Y. (2011) ABCB5 identifies a therapy-refractory tumor cell population in colorectal cancer patients. *Cancer Res.* **71**, 5307–5316 [CrossRef Medline](#)
- Gazzaniga, P., Cigna, E., Panasiti, V., Devirgiliis, V., Bottoni, U., Vincenzi, B., Nicolazzo, C., Petracca, A., and Gradilone, A. (2010) CD133 and ABCB5 as stem cell markers on sentinel lymph node from melanoma patients. *Eur. J. Surg. Oncol.* **36**, 1211–1214 [CrossRef Medline](#)
- El-Khattouti, A., Sheehan, N. T., Monico, J., Drummond, H. A., Haikel, Y., Brodell, R. T., Megahed, M., and Hassan, M. (2015) CD133⁺ melanoma subpopulation acquired resistance to caffeic acid phenethyl ester-induced apoptosis is attributed to the elevated expression of ABCB5: significance for melanoma treatment. *Cancer Lett.* **357**, 83–104 [CrossRef Medline](#)
- Frank, N. Y., Margaryan, A., Huang, Y., Schatton, T., Waaga-Gasser, A. M., Gasser, M., Sayegh, M. H., Sadee, W., and Frank, M. H. (2005) ABCB5-mediated doxorubicin transport and chemoresistance in human malignant melanoma. *Cancer Res.* **65**, 4320–4333 [CrossRef Medline](#)
- Lai, C. Y., Schwartz, B. E., and Hsu, M. Y. (2012) CD133⁺ melanoma subpopulations contribute to perivascular niche morphogenesis and tumorigenicity through vasculogenic mimicry. *Cancer Res.* **72**, 5111–5118 [CrossRef Medline](#)
- Luna, J. I., Grossenbacher, S. K., Sturgill, I. R., Ames, E., Judge, S. J., Bouzid, L. A., Darrow, M. A., Murphy, W. J., and Canter, R. J. (2019) Bortezomib augments natural killer cell targeting of stem-like tumor cells. *Cancers (Basel)* **11**, E85 [CrossRef Medline](#)
- Schatton, T., Murphy, G. F., Frank, N. Y., Yamaura, K., Waaga-Gasser, A. M., Gasser, M., Zhan, Q., Jordan, S., Duncan, L. M., Weishaupt, C., Fuhlbrigge, R. C., Kupper, T. S., Sayegh, M. H., and Frank, M. H. (2008) Identification of cells initiating human melanomas. *Nature* **451**, 345–349 [CrossRef Medline](#)
- Cheung, S. T., Cheung, P. F., Cheng, C. K., Wong, N. C., and Fan, S. T. (2011) Granulin-epithelin precursor and ATP-dependent binding cassette (ABC)B5 regulate liver cancer cell chemoresistance. *Gastroenterology* **140**, 344–355 [CrossRef Medline](#)
- Grimm, M., Krimmel, M., Polligkeit, J., Alexander, D., Munz, A., Kluba, S., Keutel, C., Hoffmann, J., Reinert, S., and Hoefert, S. (2012) ABCB5 expression and cancer stem cell hypothesis in oral squamous cell carcinoma. *Eur. J. Cancer* **48**, 3186–3197 [CrossRef Medline](#)
- Jongkhajornpong, P., Nakamura, T., Sotozono, C., Nagata, M., Inatomi, T., and Kinoshita, S. (2016) Elevated expression of ABCB5 in ocular surface squamous neoplasia. *Sci. Rep.* **6**, 20541 [CrossRef Medline](#)
- Kleffel, S., Lee, N., Lezcano, C., Wilson, B. J., Sobolewski, K., Saab, K. R., Mueller, H., Zhan, Q., Posch, C., Elco, C. P., DoRosario, A., Garcia, S. S., Thakuria, M., Wang, Y. E., Wang, L. C., et al. (2016) ABCB5-targeted chemoresistance reversal inhibits Merkel cell carcinoma growth. *J. Invest. Dermatol.* **136**, 838–846 [CrossRef Medline](#)
- Bowman, R. L., Wang, Q., Carro, A., Verhaak, R. G., and Squatrito, M. (2017) GlioVis data portal for visualization and analysis of brain tumor expression datasets. *Neuro Oncol.* **19**, 139–141 [CrossRef Medline](#)

ABCB5 targeting sensitizes GBM to temozolomide treatment

30. Scherer, H. J. (1940) A critical review: the pathology of cerebral gliomas. *J. Neurol. Psychiatry* **3**, 147–177 [CrossRef Medline](#)
31. Verhaak, R. G., Hoadley, K. A., Purdom, E., Wang, V., Qi, Y., Wilkerson, M. D., Miller, C. R., Ding, L., Golub, T., Mesirov, J. P., Alexe, G., Lawrence, M., O’Kelly, M., Tamayo, P., Weir, B. A., *et al.* (2010) Integrated genomic analysis identifies clinically relevant subtypes of glioblastoma characterized by abnormalities in PDGFRA, IDH1, EGFR, and NF1. *Cancer Cell* **17**, 98–110 [CrossRef Medline](#)
32. Olar, A., and Aldape, K. D. (2014) Using the molecular classification of glioblastoma to inform personalized treatment. *J. Pathol.* **232**, 165–177 [CrossRef Medline](#)
33. Behnan, J., Finocchiaro, G., and Hanna, G. (2019) The landscape of the mesenchymal signature in brain tumours. *Brain* **142**, 847–866 [CrossRef Medline](#)
34. Pore, N., Liu, S., Haas-Kogan, D. A., O’Rourke, D. M., and Maity, A. (2003) PTEN mutation and epidermal growth factor receptor activation regulate vascular endothelial growth factor (VEGF) mRNA expression in human glioblastoma cells by transactivating the proximal VEGF promoter. *Cancer Res.* **63**, 236–241 [Medline](#)
35. Ksander, B. R., Kolovou, P. E., Wilson, B. J., Saab, K. R., Guo, Q., Ma, J., McGuire, S. P., Gregory, M. S., Vincent, W. J., Perez, V. L., Cruz-Guilloty, F., Kao, W. W., Call, M. K., Tucker, B. A., Zhan, Q., *et al.* (2014) ABCB5 is a limbal stem cell gene required for corneal development and repair. *Nature* **511**, 353–357 [CrossRef Medline](#)
36. Frank, N. Y., Pendse, S. S., Lapchak, P. H., Margaryan, A., Shlain, D., Doeing, C., Sayegh, M. H., and Frank, M. H. (2003) Regulation of progenitor cell fusion by ABCB5 P-glycoprotein, a novel human ATP-binding cassette transporter. *J. Biol. Chem.* **278**, 47156–47165 [CrossRef Medline](#)
37. Singh, S. K., Clarke, I. D., Terasaki, M., Bonn, V. E., Hawkins, C., Squire, J., and Dirks, P. B. (2003) Identification of a cancer stem cell in human brain tumors. *Cancer Res.* **63**, 5821–5828 [Medline](#)
38. Wei, L. H., Su, H., Hildebrandt, I. J., Phelps, M. E., Czernin, J., and Weber, W. A. (2008) Changes in tumor metabolism as readout for mammalian target of rapamycin kinase inhibition by rapamycin in glioblastoma. *Clin. Cancer Res.* **14**, 3416–3426 [CrossRef Medline](#)
39. Shah, M. A., and Schwartz, G. K. (2001) Cell cycle-mediated drug resistance: an emerging concept in cancer therapy. *Clin. Cancer Res.* **7**, 2168–2181 [Medline](#)
40. Alonso, M. M., Gomez-Manzano, C., Bekele, B. N., Yung, W. K., and Fueyo, J. (2007) Adenovirus-based strategies overcome temozolomide resistance by silencing the O6-methylguanine-DNA methyltransferase promoter. *Cancer Res.* **67**, 11499–11504 [CrossRef Medline](#)
41. Hemmati, H. D., Nakano, I., Lazareff, J. A., Masterman-Smith, M., Geschwind, D. H., Bronner-Fraser, M., and Kornblum, H. I. (2003) Cancerous stem cells can arise from pediatric brain tumors. *Proc. Natl. Acad. Sci. U.S.A.* **100**, 15178–15183 [CrossRef Medline](#)
42. Auffinger, B., Tobias, A. L., Han, Y., Lee, G., Guo, D., Dey, M., Lesniak, M. S., and Ahmed, A. U. (2014) Conversion of differentiated cancer cells into cancer stem-like cells in a glioblastoma model after primary chemotherapy. *Cell Death Differ.* **21**, 1119–1131 [CrossRef Medline](#)
43. Woo, J. Y., Yang, S. H., Lee, Y. S., Lee, S. Y., Kim, J., and Hong, Y. K. (2015) Continuous low-dose temozolomide chemotherapy and microvessel density in recurrent glioblastoma. *J. Korean Neurosurg. Soc.* **58**, 426–431 [CrossRef Medline](#)
44. Flatten, K., Dai, N. T., Vroman, B. T., Loegering, D., Erlichman, C., Karnitz, L. M., and Kaufmann, S. H. (2005) The role of checkpoint kinase 1 in sensitivity to topoisomerase I poisons. *J. Biol. Chem.* **280**, 14349–14355 [CrossRef Medline](#)
45. Lin, F., de Gooijer, M. C., Roig, E. M., Buil, L. C., Christner, S. M., Beumer, J. H., Würdinger, T., Beijnen, J. H., and van Tellingen, O. (2014) ABCB1, ABCG2, and PTEN determine the response of glioblastoma to temozolomide and ABT-888 therapy. *Clin. Cancer Res.* **20**, 2703–2713 [CrossRef Medline](#)
46. Wijaya, J., Fukuda, Y., and Schuetz, J. D. (2017) Obstacles to brain tumor therapy: key ABC transporters. *Int. J. Mol. Sci.* **18**, E2544 [CrossRef Medline](#)
47. Munoz, J. L., Walker, N. D., Scotto, K. W., and Rameshwar, P. (2015) Temozolomide competes for P-glycoprotein and contributes to chemoresistance in glioblastoma cells. *Cancer Lett.* **367**, 69–75 [CrossRef Medline](#)
48. Guo, Q., Grimmig, T., Gonzalez, G., Giobbie-Hurder, A., Berg, G., Carr, N., Wilson, B. J., Banerjee, P., Ma, J., Gold, J. S., Nandi, B., Huang, Q., Waaga-Gasser, A. M., Lian, C. G., Murphy, G. F., *et al.* (2018) ATP-binding cassette member B5 (ABCB5) promotes tumor cell invasiveness in human colorectal cancer. *J. Biol. Chem.* **293**, 11166–11178 [CrossRef Medline](#)
49. Carvalho, B. S., and Irizarry, R. A. (2010) A framework for oligonucleotide microarray preprocessing. *Bioinformatics* **26**, 2363–2367 [CrossRef Medline](#)
50. Bolstad, B. M., Irizarry, R. A., Astrand, M., and Speed, T. P. (2003) A comparison of normalization methods for high density oligonucleotide array data based on variance and bias. *Bioinformatics* **19**, 185–193 [CrossRef Medline](#)
51. Irizarry, R. A., Hobbs, B., Collin, F., Beazer-Barclay, Y. D., Antonellis, K. J., Scherf, U., and Speed, T. P. (2003) Exploration, normalization, and summaries of high density oligonucleotide array probe level data. *Biostatistics* **4**, 249–264 [CrossRef Medline](#)
52. Krämer, A., Green, J., Pollard, J., Jr., and Tugendreich, S. (2014) Causal analysis approaches in Ingenuity Pathway Analysis. *Bioinformatics* **30**, 523–530 [CrossRef Medline](#)
53. Zhang, Z., Miao, L., Lv, C., Sun, H., Wei, S., Wang, B., Huang, C., and Jiao, B. (2013) Wentilactone B induces G₂/M phase arrest and apoptosis via the Ras/Raf/MAPK signaling pathway in human hepatoma SMMC-7721 cells. *Cell Death Dis.* **4**, e657 [CrossRef Medline](#)